www.cad-journal.net
Computer-Aided Design AND APPLICATIONS™

Triarc Curves

Tom Guo[1]

[1]Independent Researcher, Toronto, Canada, tguoyaar@gmail.com

Corresponding author: Tom Guo, tguoyaar@gmail.com

Abstract. A triarc is a composite curve of three circular arcs, where the middle arc joins the two side arcs tangentially, and the two side arcs match the two endpoints and their associated tangents. This paper presents a new trigonometric and algebraic method for constructing G^1 continuous triarc curves. The triarc is constructed within a triangle such that each side arc is tangent to one edge of the triangle, and the middle arc connects both side arcs tangentially. Three types of C-shaped triarcs are defined based on the tangency relationships between the middle and side arcs. A hierarchy of approach and anti-approach properties (general, strict, advanced) is formally introduced. Approach theorems are established and rigorously proven for the strict and advanced cases. A complete set of equations is derived for calculating the arc radii, utilizing three approach coefficients $(\alpha_0, \alpha_1, \alpha_2)$ that serve as independent shape control parameters controlling the triarc's shape relative to the two-edge control polyline of the triangle. The proposed construction method enables fine and robust shape control of triarc families. Several examples demonstrate the robust monotonic behavior of these triarc families, indicating their suitability for precision geometric modeling and CNC applications.

Keywords: triarc, biarc, circular arc curve, shape control, approach mode
DOI: https://doi.org/10.14733/cadaps.2026.679-724

1 INTRODUCTION

Circular arcs are fundamental in CAD/CAM and CAGD systems and are extensively used in design and manufacturing. A circular arc spline is a curve composed of multiple circular arcs and/or straight-line segments joined tangentially, where a straight-line segment is a special case of a circular arc with an infinite radius. Although a circular arc spline is only G^1 continuous, it possesses several desirable geometric properties:

- Each circular arc has constant curvature.
- The length of a circular arc can be computed exactly in closed form.
- The rotation of a circular arc preserves its intrinsic geometric properties (length and constant curvature).
- An offset circular arc is still a circular arc.

- The offset of a circular arc spline remains a circular arc spline; however, inward offsets may generate additional self-intersections or cusps depending on the offset distance.
- Circular arcs have simple parametric representations, and their intersections are geometrically well-defined.

Circular arc curves have been widely studied for applications in geometric design, geometric modeling, and curve fitting [1, 3, 4, 5, 7, 8, 2]. Early work introduced biarc curves [3] and studied the geometry of piecewise circular curves [1], followed by geometric formulations of planar biarcs [4]. Arc spline approximation methods were developed for smooth planar curves [7, 5], with applications to data fitting and engineering design [8]. More recent work has focused on robust and stable biarc computation [2], while broader developments in geometric modeling and approximation have been surveyed in [6]. Many of these studies focus on circular arc splines constructed from biarcs. Triarc-based constructions have also been investigated for practical engineering applications. In particular, Yang [9] proposed an iterative triarc fitting algorithm for CNC machining of cam profiles. Biarcs are simple and widely used, but they are limited by a restricted parameter space (one degree of freedom) and may fail to exist for certain endpoint configurations. Triarcs, by contrast, have two degrees of freedom, which provide increased flexibility, guarantee the existence of a solution, and enable satisfaction of higher-order continuity requirements such as G^2 curvature matching. In this work, the flexibility is achieved through shape control using the approach coefficients $(\alpha_0, \alpha_1, \alpha_2)$.

Compared with biarc constructions, triarcs provide an additional degree of freedom which increases geometric flexibility. Consequently, the triarc framework allows greater shape control and a broader range of predictable monotone approach behavior relative to the control polyline, which is more limited in biarc constructions.

This paper presents a method for constructing triarcs that possess monotonic approach and anti-approach properties. Trigonometry and algebra are used to derive a set of equations for determining the radii of the middle and side circular arcs. Three approach coefficients, α_0, α_1, and α_2, are introduced as shape control parameters, allowing for fine control of the triarc geometry and its proximity to the two-edge control polyline of the control triangle.

A triarc is defined as a curve segment composed of three circular arcs, where the middle arc joins the two side arcs tangentially and the side arcs match the endpoints and their tangents. Some of these arcs may degenerate into straight-line segments. In terms of inflection, triarcs can be classified into three types: non-inflection (C-shaped), single-inflection (S-shaped), and double-inflection (double S-shaped). Non-inflection triarcs preserve convexity, making them ideal for robust geometric approximation in practical tasks such as CNC toolpaths, CAD curve design, and shape-preserving interpolation, where avoiding unwanted oscillations is critical. Non-inflection triarcs can be either self-intersecting or non-self-intersecting; this paper focuses on constructing non-self-intersecting C-shaped triarcs within a triangle.

The remainder of the paper is organized as follows. Section 2 presents the triarc construction method for the three types of C-shaped triarcs within $\triangle ABC$. Section 3 introduces the approach and anti-approach concepts and proves the approach theorems for **Type 1**, **Type 2**, and **Type 3** triarcs. Section 4 provides examples validating these theorems. Section 5 summarizes the findings. Appendix A provides auxiliary methods used for computing boundary radii that support the triarc construction process. Appendix B provides lemmas used for constructing the middle arc radius R_1 and for proving the one-factor strict approach theorem of R_1 (Theorem 3.1).

A right-handed coordinate system is used throughout this paper, and the following symbols are applied:

- $\nearrow$ (denotes increases).
- $\searrow$ (denotes decreases).

2 TRIARC CONSTRUCTION

C-shaped triarcs are constructed within a triangle. As shown in Fig. 1, AB and BC are two edges of $\triangle ABC$. Based on the cross product and the relative lengths of the edge vectors $\overrightarrow{\mathbf{AB}}$ and $\overrightarrow{\mathbf{BC}}$, six types of triangles can be classified, without considering the edge $\overrightarrow{\mathbf{CA}}$:

- $\overrightarrow{\mathbf{AB}} \times \overrightarrow{\mathbf{BC}} < 0$ and $|\overrightarrow{\mathbf{AB}}| < |\overrightarrow{\mathbf{BC}}|$ (Fig. 1a).
- $\overrightarrow{\mathbf{AB}} \times \overrightarrow{\mathbf{BC}} < 0$ and $|\overrightarrow{\mathbf{AB}}| > |\overrightarrow{\mathbf{BC}}|$ (Fig. 1b).
- $\overrightarrow{\mathbf{AB}} \times \overrightarrow{\mathbf{BC}} < 0$ and $|\overrightarrow{\mathbf{AB}}| = |\overrightarrow{\mathbf{BC}}|$ (Fig. 1c).
- $\overrightarrow{\mathbf{AB}} \times \overrightarrow{\mathbf{BC}} > 0$ and $|\overrightarrow{\mathbf{AB}}| < |\overrightarrow{\mathbf{BC}}|$ (Fig. 1d).
- $\overrightarrow{\mathbf{AB}} \times \overrightarrow{\mathbf{BC}} > 0$ and $|\overrightarrow{\mathbf{AB}}| > |\overrightarrow{\mathbf{BC}}|$ (Fig. 1e).
- $\overrightarrow{\mathbf{AB}} \times \overrightarrow{\mathbf{BC}} > 0$ and $|\overrightarrow{\mathbf{AB}}| = |\overrightarrow{\mathbf{BC}}|$ (Fig. 1f).

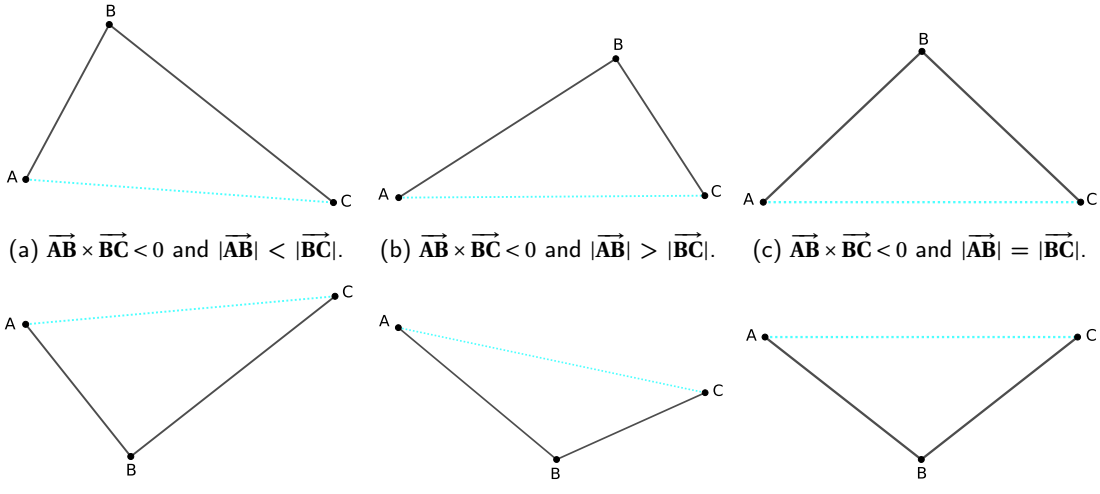

(a) $\overrightarrow{\mathbf{AB}} \times \overrightarrow{\mathbf{BC}} < 0$ and $|\overrightarrow{\mathbf{AB}}| < |\overrightarrow{\mathbf{BC}}|$. (b) $\overrightarrow{\mathbf{AB}} \times \overrightarrow{\mathbf{BC}} < 0$ and $|\overrightarrow{\mathbf{AB}}| > |\overrightarrow{\mathbf{BC}}|$. (c) $\overrightarrow{\mathbf{AB}} \times \overrightarrow{\mathbf{BC}} < 0$ and $|\overrightarrow{\mathbf{AB}}| = |\overrightarrow{\mathbf{BC}}|$.

(d) $\overrightarrow{\mathbf{AB}} \times \overrightarrow{\mathbf{BC}} > 0$ and $|\overrightarrow{\mathbf{AB}}| < |\overrightarrow{\mathbf{BC}}|$. (e) $\overrightarrow{\mathbf{AB}} \times \overrightarrow{\mathbf{BC}} > 0$ and $|\overrightarrow{\mathbf{AB}}| > |\overrightarrow{\mathbf{BC}}|$. (f) $\overrightarrow{\mathbf{AB}} \times \overrightarrow{\mathbf{BC}} > 0$ and $|\overrightarrow{\mathbf{AB}}| = |\overrightarrow{\mathbf{BC}}|$.

Figure 1: Six types of triangles without consideration of edge $\overrightarrow{\mathbf{CA}}$.

Without loss of generality, for non-isosceles triangles, only the type of triangle ($\overrightarrow{\mathbf{AB}} \times \overrightarrow{\mathbf{BC}} < 0$ and $|\overrightarrow{\mathbf{AB}}| < |\overrightarrow{\mathbf{BC}}|$) in Fig. 1a is discussed, as all the other types of non-isosceles triangles can be converted to this type through coordinate transformations (reflection or rotation); for isosceles triangles, only the type of triangle ($\overrightarrow{\mathbf{AB}} \times \overrightarrow{\mathbf{BC}} < 0$ and $|\overrightarrow{\mathbf{AB}}| = |\overrightarrow{\mathbf{BC}}|$) in Fig. 1c is discussed for the same reason.

Fig. 2 illustrates that within $\triangle ABC$, the side circular arc $\widehat{A4}$ on side circle 0, the middle circular arc $\widehat{45}$ on middle circle 1, and the side circular arc $\widehat{5C}$ on side circle 2 construct a triarc $\widehat{A45C}$ that matches two endpoints, A and C, and two end tangents, $\overrightarrow{\mathbf{AB}}$ and $\overrightarrow{\mathbf{CB}}$. A C-shaped triarc constructed within a given $\triangle ABC$ meets these conditions:

1. A middle circular arc and two side circular arcs construct a triarc; and these three circular arcs are minor arcs that lie inside $\triangle ABC$.

2. It is G^1 continuous as the middle circular arc connects the two side circular arcs tangentially.

3. One side circular arc matches point A and is tangent to edge AB at A; the other side circular arc matches point C and is tangent to edge BC at C.
4. It is non-self-intersecting.
5. There is no inflection on the triarc.
6. It is convexity-preserving in shape.

2.1 Three Types of C-Shaped Triarcs

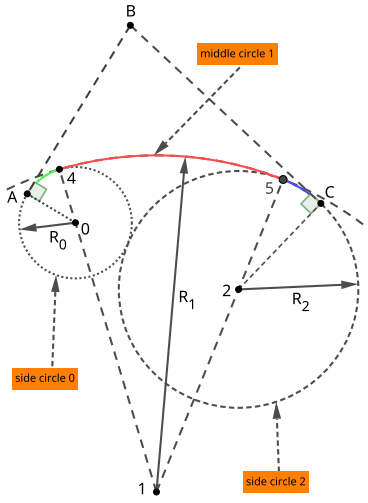

(a) **Type 1 C-shaped triarc:** Both side circles 0 and 2 are internally tangent to middle circle 1 at the points 4 and 5, respectively.

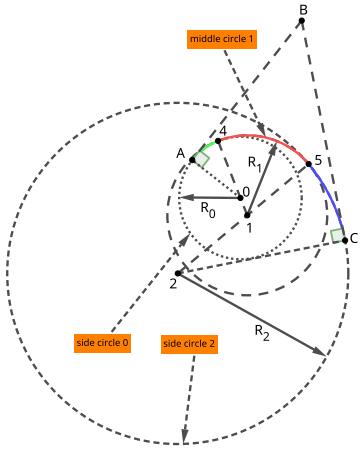

(b) **Type 2 C-shaped triarc:** Side circle 0 is internally tangent to middle circle 1 at the point 4 and middle circle 1 is internally tangent to side circle 2 at the point 5.

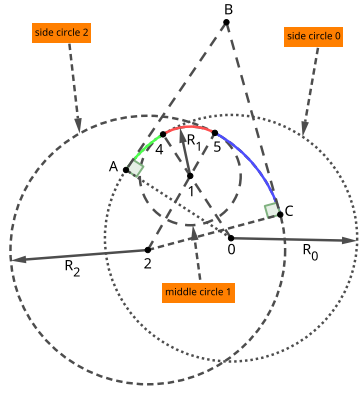

(c) **Type 3 C-shaped triarc:** Middle circle 1 is internally tangent to both side circles 0 and 2 at the points 4 and 5, respectively.

Figure 2: Three types of C-shaped triarcs are constructed within $\triangle ABC$. Side circle 0 is tangent to AB at point A and side circle 2 is tangent to BC at point C. Middle circle 1 is tangent to both side circles 0 and 2 at the tangent points 4 and 5, respectively. $\overset{\frown}{A45C}$ is a triarc ($\overset{\frown}{A4} + \overset{\frown}{45} + \overset{\frown}{5C}$) in which the side circular arc $\overset{\frown}{A4}$ is on side circle 0, the middle circular arc $\overset{\frown}{45}$ is on middle circle 1, and the side circular arc $\overset{\frown}{5C}$ is on side circle 2. $\overset{\frown}{45}$ is tangent to $\overset{\frown}{A4}$ at point 4 and to $\overset{\frown}{5C}$ at point 5. $\overset{\frown}{A4}$, $\overset{\frown}{45}$, and $\overset{\frown}{5C}$ are minor circular arcs.

As depicted in Fig. 2, the triarc $\overset{\frown}{A45C}$ is constructed within $\triangle ABC$ from three minor circular arcs with radii R_0 ($\overset{\frown}{A4}$), R_1 ($\overset{\frown}{45}$), and R_2 ($\overset{\frown}{5C}$). Both tangent points 4 and 5 lie inside $\triangle ABC$.

Three types of C-shaped triarcs are defined by the tangency relationships between the middle circular arc $\overset{\frown}{45}$ and the two side circular arcs $\overset{\frown}{A4}$ and $\overset{\frown}{5C}$:

- **Type 1 C-shaped triarc** (Fig. 2a): Both side circular arcs $\overset{\frown}{A4}$ and $\overset{\frown}{5C}$ are internally tangent to the middle circular arc $\overset{\frown}{45}$.
- **Type 2 C-shaped triarc** (Fig. 2b): The side circular arc $\overset{\frown}{A4}$ is internally tangent to the middle circular arc $\overset{\frown}{45}$ that is internally tangent to the side circular arc $\overset{\frown}{5C}$.

- **Type 3 C-shaped triarc** (Fig. 2c): The middle circular arc $\widehat{45}$ is internally tangent to both the side circular arcs $\widehat{A4}$ and $\widehat{5C}$.

Table 1 summarizes the relationships among the three types of C-shaped triarcs and their corresponding radii and curvature characteristics.

Table 1: Relationships among the three types of C-shaped triarcs, their radius hierarchies, and curvature characteristics.

Type	Tangency Relation	Radius Relation	Curvature Relation
Type 1	Side arcs $\widehat{A4}$ and $\widehat{5C}$ are internally tangent to the middle arc $\widehat{45}$.	$R_1 > R_0$, $R_1 > R_2$	$\kappa_1 < \kappa_0$, $\kappa_1 < \kappa_2$
Type 2	$\widehat{A4}$ is internally tangent to $\widehat{45}$, which is internally tangent to $\widehat{5C}$.	$R_2 > R_1 > R_0$	$\kappa_2 < \kappa_1 < \kappa_0$
Type 3	The middle arc $\widehat{45}$ is internally tangent to both side arcs $\widehat{A4}$ and $\widehat{5C}$.	$R_0 > R_1$, $R_2 > R_1$	$\kappa_1 > \kappa_0$, $\kappa_1 > \kappa_2$

Note. κ_i denotes the curvature of the circular arc with radius R_i ($\kappa_i = 1/R_i$).

2.2 Construction of Radii R_0 and R_2 (Side Circles)

In $\triangle ABC$, R_0 and R_2 are the radii of side circles 0 and 2, respectively. The approach coefficients α_0 and α_2 serve as shape control parameters that define R_0 and R_2. Adjusting these coefficients modifies R_0 and R_2, thereby influencing the curvature and overall geometry of the C-shaped triarcs. The algebraic relations $R_0(\alpha_0)$ and $R_2(\alpha_2)$ are derived in the following subsections.

Radius R_0 is constructed such that increasing α_0 enlarges R_0 and brings the triarc closer to edge AB, while decreasing α_0 moves it farther away. Similarly, R_2 is constructed so that increasing α_2 enlarges R_2 and brings the triarc closer to edge BC, whereas decreasing α_2 moves it farther away.

For the three types of C-shaped triarcs, the coefficients α_0 and α_2 are defined as follows:

- **Type 1 C-shaped triarc**: $0 < \alpha_0 < 3$, $0 < \alpha_2 < 3$.
- **Type 2 C-shaped triarc**: $3 < \alpha_0 < 6$, $3 < \alpha_2 < +\infty$.
- **Type 3 C-shaped triarc**: $6 \le \alpha_0 < +\infty$, $6 < \alpha_2 < +\infty$.

In all cases, side circles 0 and 2 are tangent to edges AB and BC at vertices A and C, respectively. In **Type 1** (Fig. 3), the two side circles are either separated or intersecting but do not contain each other. In **Type 2** (Fig. 4), circle 0 is contained within circle 2 without touching it. In **Type 3** (Fig. 5), the two side circles intersect. These geometric relationships establish the framework for constructing R_0 and R_2 in the following subsections.

2.2.1 Construction of Radii R_0 and R_2 for Type 1 C-Shaped Triarcs

As depicted in Fig. 3a, the center 0 of side circle 0 is constrained by the inequality $\overrightarrow{\mathbf{BH}} \times \overrightarrow{\mathbf{H0}} < 0$, or equivalently,

$$0 < R_0 < |\overrightarrow{\mathbf{AB}}| \cdot \tan(\varphi), \quad \text{where } \varphi \text{ is the half-angle of } \angle\text{ABC}. \tag{1}$$

The center 2 of side circle 2 is constrained by the inequality $\overrightarrow{\mathbf{EF}} \times \overrightarrow{\mathbf{F2}} > 0$. Therefore, R_2 is bounded by R_0 within the following range:

$$0 < R_2 < \frac{|\overrightarrow{\mathbf{EI}}|}{\cos(\beta)} + R_0, \quad \text{where } \beta \text{ is } \angle\text{EIF}. \tag{2}$$

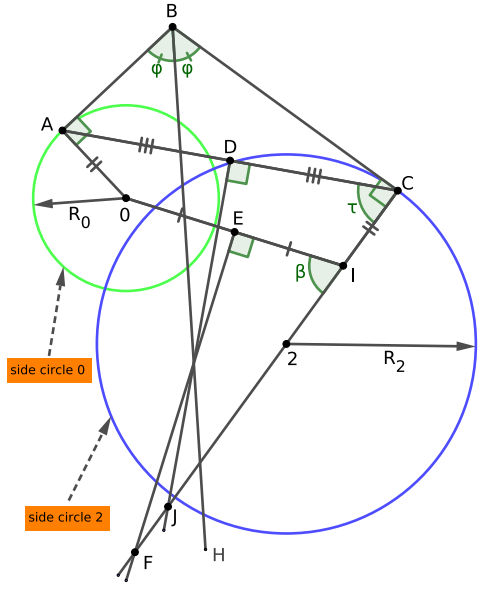

(a) **Type 1:** $|\overrightarrow{\mathbf{AB}}| < |\overrightarrow{\mathbf{BC}}|$. R_0 = the radius of side circle 0, R_2 = the radius of side circle 2, IC=A0=R_0, AD=DC, AC⊥DJ, 0E=EI, 0I⊥EF, BH is the bisector of ∠ABC, $\overrightarrow{\mathbf{BH}} \times \overrightarrow{\mathbf{H0}} < 0$, and $\overrightarrow{\mathbf{EF}} \times \overrightarrow{\mathbf{F2}} > 0$.

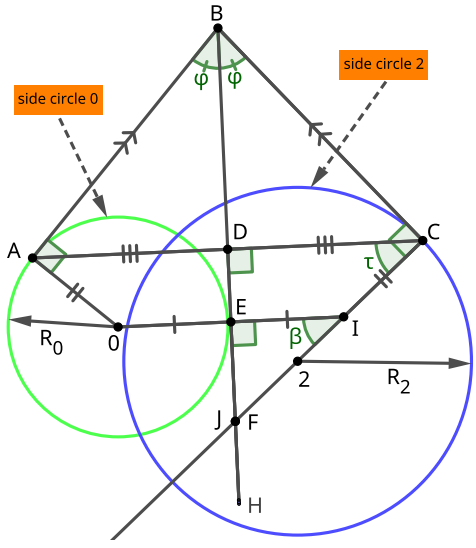

(b) **Type 1:** $|\overrightarrow{\mathbf{AB}}| = |\overrightarrow{\mathbf{BC}}|$. R_0 = the radius of side circle 0, R_2 = the radius of side circle 2, IC=A0=R_0, AD=DC, AC⊥DJ, 0E=EI, 0I⊥EF, BH is the bisector of ∠ABC, $\overrightarrow{\mathbf{BH}} \times \overrightarrow{\mathbf{H0}} < 0$, and $\overrightarrow{\mathbf{BH}} \times \overrightarrow{\mathbf{H2}} > 0$.

Figure 3: **Type 1: $\mathbf{R_0}$ and $\mathbf{R_2}$ Construction**. R_0 and R_2 are defined for **Type 1** C-shaped triarcs in $\triangle ABC$. Side circles 0 and 2 are either separated or intersecting but do not contain each other.

Inequalities (1) and (2) ensure that side circles 0 and 2 are either separated or intersecting but do not contain each other, allowing for the successful construction of **Type 1** C-shaped triarcs. To construct a family of **Type 1** C-shaped triarcs, the approach coefficients α_0 and α_2 are introduced into the formulas for R_0 and R_2, respectively:

$$R_0 = \frac{\alpha_0}{3} \cdot |\overrightarrow{\mathbf{AB}}| \cdot \tan(\varphi), \quad (0 < \alpha_0 < 3), \quad \text{where } \varphi \text{ is the half-angle of } \angle\text{ABC}. \tag{3a}$$

$$R_2 = \frac{\alpha_2}{3} \cdot \left(\frac{|\overrightarrow{\mathbf{EI}}|}{\cos(\beta)} + R_0 \right), \quad (0 < \alpha_2 < 3), \quad \text{where } \beta \text{ is } \angle\text{EIF}. \tag{3b}$$

Eqs. (3a) and (3b) satisfy inequalities (1) and (2), respectively.

The process of constructing R_0 and R_2 involves the following steps: first, R_0 is calculated using α_0 in Eq. (3a); and second, R_2 is calculated using α_2 in Eq. (3b) after R_0 is given in Eq. (3a).

For the special case where $|\overrightarrow{\mathbf{AB}}| = |\overrightarrow{\mathbf{BC}}|$ (Fig. 3b), the same Eqs. (3a) and (3b) apply.

2.2.2 Construction of Radii $\mathbf{R_0}$ and $\mathbf{R_2}$ for Type 2 C-Shaped Triarcs

As depicted in Fig. 4a, the center 0 of side circle 0 must satisfy the inequality $\overrightarrow{\mathbf{BH}} \times \overrightarrow{\mathbf{H0}} < 0$, meaning that the radius R_0 must be in the range:

$$0 < R_0 < |\overrightarrow{\mathbf{AB}}| \cdot \tan(\varphi), \quad \text{where } \varphi \text{ is the half-angle of } \angle\text{ABC}. \tag{4}$$

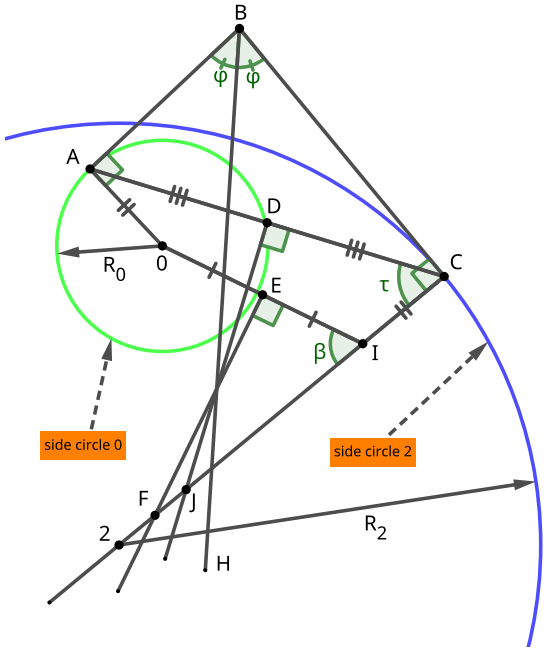

(a) **Type 2:** $|\overrightarrow{\mathbf{AB}}| < |\overrightarrow{\mathbf{BC}}|$. R_0 = the radius of side circle 0, R_2 = the radius of side circle 2, IC=A0=R_0, AD=DC, AC⊥DJ, 0E=EI, 0I⊥EF, BH is the bisector of ∠ABC, $\overrightarrow{\mathbf{BH}} \times \overrightarrow{\mathbf{H0}} < 0$, and $\overrightarrow{\mathbf{EF}} \times \overrightarrow{\mathbf{F2}} < 0$.

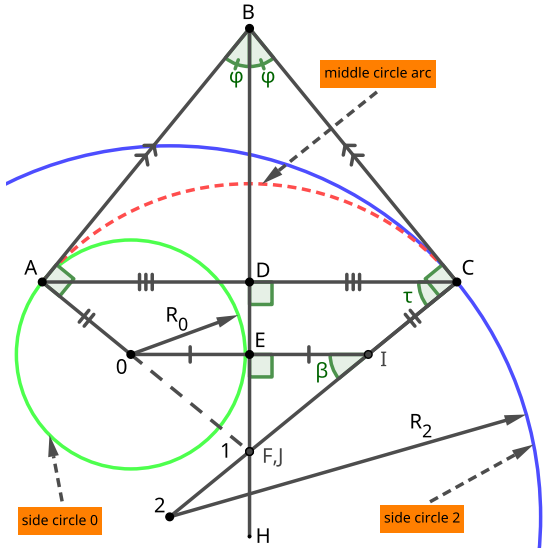

(b) **Type 2:** $|\overrightarrow{\mathbf{AB}}| = |\overrightarrow{\mathbf{BC}}|$. R_0 = the radius of side circle 0, R_2 = the radius of side circle 2, BH is the bisector of ∠ABC, $\overrightarrow{\mathbf{BH}} \times \overrightarrow{\mathbf{H0}} < 0$, and $\overrightarrow{\mathbf{EF}} \times \overrightarrow{\mathbf{F2}} < 0$.

Figure 4: **Type 2: $\mathbf{R_0}$ and $\mathbf{R_2}$ Construction**. R_0 and R_2 are defined for **Type 2** C-shaped triarcs in $\triangle ABC$. Side circle 2 contains side circle 0 without touching it.

The center 2 of side circle 2 must satisfy the inequality $\overrightarrow{\mathbf{EF}} \times \overrightarrow{\mathbf{F2}} < 0$. Therefore, R_2 is restricted by R_0 within this range:

$$\frac{|\overrightarrow{\mathbf{EI}}|}{\cos(\beta)} + R_0 < R_2 < +\infty, \quad \text{where } \beta \text{ is } \angle\text{EIF}. \tag{5}$$

Inequalities (4) and (5) ensure that side circle 2 contains side circle 0 without touching it, allowing for the successful construction of **Type 2** C-shaped triarcs. Thus, to construct a family of **Type 2** C-shaped triarcs, the approach coefficients α_0 and α_2 are introduced into the formulas for R_0 and R_2, respectively:

$$R_0 = \frac{\alpha_0 - 3}{3} \cdot |\overrightarrow{\mathbf{AB}}| \cdot \tan(\varphi), \quad (3 < \alpha_0 < 6), \quad \text{where } \varphi \text{ is the half-angle of } \angle\text{ABC}. \tag{6a}$$

$$R_2 = e^{(\alpha_2 - 3)} \cdot \left(\frac{|\overrightarrow{\mathbf{EI}}|}{\cos(\beta)} + R_0 \right), \quad (3 < \alpha_2 < +\infty), \quad \text{where } \beta \text{ is } \angle\text{EIF}. \tag{6b}$$

Eqs. (6a) and (6b) satisfy inequalities (4) and (5), respectively.

The process of constructing R_0 and R_2 involves these steps: first, R_0 is calculated using α_0 in Eq. (6a); and second, R_2 is calculated using α_2 in Eq. (6b) after R_0 is given in Eq. (6a).

For the special case where $|\overrightarrow{\mathbf{AB}}| = |\overrightarrow{\mathbf{BC}}|$ (Fig. 4b), a **Type 2** C-shaped triarc degenerates to a single circular

arc with radius $|\overrightarrow{\mathbf{AB}}|\cdot\tan(\varphi)$ connecting points A and C for any combination of R_0 and R_2 calculated by Eqs. (6a) and (6b).

2.2.3 Construction of Radii $\mathbf{R_0}$ and $\mathbf{R_2}$ for Type 3 C-Shaped Triarcs

For **Type 3** C-shaped triarcs constructed within $\triangle ABC$ where $|\overrightarrow{\mathbf{AB}}| \le |\overrightarrow{\mathbf{BC}}|$, two scenarios are identified based on the constraint on center 0:

- $\overrightarrow{\mathbf{BH}} \times \overrightarrow{\mathbf{H0}} < 0$ (Fig. 5a and Fig. 5c).
- $\overrightarrow{\mathbf{BH}} \times \overrightarrow{\mathbf{H0}} \ge 0$ (Fig. 5b and Fig. 5d).

2.2.3.1 Construction of Radii $\mathbf{R_0}$ and $\mathbf{R_2}$ for $\overrightarrow{\mathbf{BH}} \times \overrightarrow{\mathbf{H0}} \le 0$ (Limited R_0)

As depicted in Fig. 5a, the center 0 of side circle 0 is constrained by the inequality $\overrightarrow{\mathbf{BH}} \times \overrightarrow{\mathbf{H0}} < 0$, or equivalently,

$$0 < R_0 < |\overrightarrow{\mathbf{AB}}| \cdot \tan(\varphi), \quad \text{where } \varphi \text{ is the half-angle of } \angle\text{ABC}. \tag{7}$$

The center 2 of side circle 2 is constrained by the inequalities $\overrightarrow{\mathbf{EF}} \times \overrightarrow{\mathbf{F2}} > 0$ and $\overrightarrow{\mathbf{DJ}} \times \overrightarrow{\mathbf{J2}} < 0$. Therefore, R_2 is bounded by R_0 within this range:

$$\frac{|\overrightarrow{\mathbf{DC}}|}{\cos(\tau)} < R_2 < \frac{|\overrightarrow{\mathbf{EI}}|}{\cos(\beta)} + R_0, \quad \text{where } \tau \text{ is } \angle\text{ACJ and } \beta \text{ is } \angle\text{EIF}. \tag{8}$$

Inequalities (7) and (8) ensure that side circle 0 intersects side circle 2, allowing for the successful construction of **Type 3** C-shaped triarcs. Thus, to construct a family of **Type 3** C-shaped triarcs, the approach coefficients α_0 and α_2 are introduced into the formulas for R_0 and R_2, respectively:

$$R_0 = e^{-\frac{1}{\alpha_0 - 6}} \cdot |\overrightarrow{\mathbf{AB}}| \cdot \tan(\varphi), \quad (6 < \alpha_0 < +\infty), \quad \text{where } \varphi \text{ is the half-angle of } \angle\text{ABC}. \tag{9a}$$

$$R_2 = \frac{|\overrightarrow{\mathbf{DC}}|}{\cos(\tau)} + e^{-\frac{1}{\alpha_2 - 6}} \cdot \left(\frac{|\overrightarrow{\mathbf{EI}}|}{\cos(\beta)} + R_0 - \frac{|\overrightarrow{\mathbf{DC}}|}{\cos(\tau)} \right), \quad (6 < \alpha_2 < +\infty), \tag{9b}$$

where τ is $\angle$ACJ and β is $\angle$EIF.

Eqs. (9a) and (9b) satisfy inequalities (7) and (8), respectively.

The process of constructing R_0 and R_2 requires these steps: first, R_0 is calculated using α_0 in Eq. (9a); and second, R_2 is calculated using α_2 in Eq. (9b) after R_0 is given in Eq. (9a).

For the special case where $|\overrightarrow{\mathbf{AB}}| = |\overrightarrow{\mathbf{BC}}|$ (Fig. 5c), $R_2 = \frac{|\overrightarrow{\mathbf{DC}}|}{\cos(\tau)}$ which is a constant by Eq. (9b). As side circle 0 is internally tangent to side circle 2 at point A, **Type 3** C-shaped triarcs cannot be constructed.

2.2.3.2 Construction of Radii $\mathbf{R_0}$ and $\mathbf{R_2}$ for $\overrightarrow{\mathbf{BH}} \times \overrightarrow{\mathbf{H0}} \ge 0$ (Unlimited R_0)

As depicted in Fig. 5b, the center 0 of side circle 0 is constrained by the inequality $\overrightarrow{\mathbf{BH}} \times \overrightarrow{\mathbf{H0}} \ge 0$, or equivalently,

$$|\overrightarrow{\mathbf{AB}}| \cdot \tan(\varphi) \le R_0 < +\infty, \quad \text{where } \varphi \text{ is the half-angle of } \angle\text{ABC}. \tag{10}$$

The center 2 of side circle 2 is constrained by the inequality $\overrightarrow{\mathbf{DJ}} \times \overrightarrow{\mathbf{J2}} < 0$, or equivalently,

$$\frac{|\overrightarrow{\mathbf{DC}}|}{\cos(\tau)} < R_2 < +\infty, \quad \text{where } \tau \text{ is } \angle\text{ACJ}. \tag{11}$$

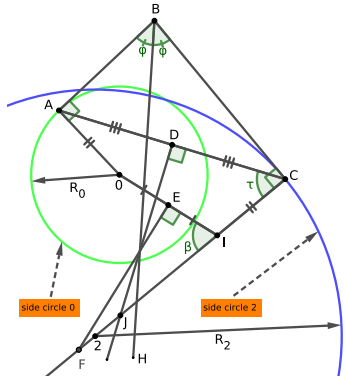

(a) **Type 3:** $|\overrightarrow{\mathbf{AB}}| < |\overrightarrow{\mathbf{BC}}|$ and $\overrightarrow{\mathbf{BH}} \times \overrightarrow{\mathbf{H0}} < 0$. R_0 = the radius of side circle 0, R_2 = the radius of side circle 2, IC=A0=R_0, AD=DC, AC⊥DJ, 0E=EI, 0I⊥EF, BH is the bisector of ∠ABC, $\overrightarrow{\mathbf{EF}} \times \overrightarrow{\mathbf{F2}} > 0$, and $\overrightarrow{\mathbf{DJ}} \times \overrightarrow{\mathbf{J2}} < 0$. $|\overrightarrow{\mathbf{02}}| < R_2$ - R_0, and side circle 0 intersects side circle 2.

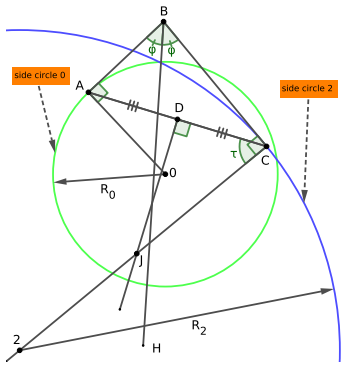

(b) **Type 3:** $|\overrightarrow{\mathbf{AB}}| < |\overrightarrow{\mathbf{BC}}|$ and $\overrightarrow{\mathbf{BH}} \times \overrightarrow{\mathbf{H0}} \geq 0$. R_0 = the radius of side circle 0, R_2 = the radius of side circle 2, A0=R_0, AD=DC, AC⊥DJ, BH is the bisector of ∠ABC, and $\overrightarrow{\mathbf{DJ}} \times \overrightarrow{\mathbf{J2}} < 0$. $|\overrightarrow{\mathbf{02}}| < R_2$ - R_0, and side circle 0 intersects side circle 2.

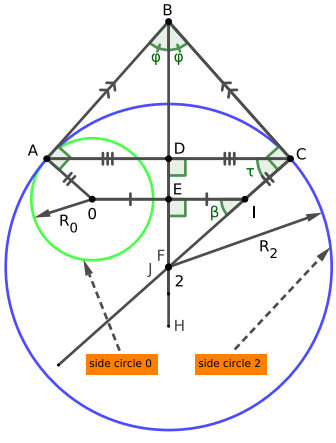

(c) **Type 3:** $|\overrightarrow{\mathbf{AB}}| = |\overrightarrow{\mathbf{BC}}|$ and $\overrightarrow{\mathbf{BH}} \times \overrightarrow{\mathbf{H0}} < 0$. R_0 = the radius of side circle 0, R_2 = the radius of side circle 2, $R_2 = \frac{|\overrightarrow{\mathbf{DC}}|}{\cos(\tau)}$, BH is the bisector of ∠ABC, and $\overrightarrow{\mathbf{BH}} \times \overrightarrow{\mathbf{H2}} = 0$. Side circle 0 is internally tangent to side circle 2 at point A.

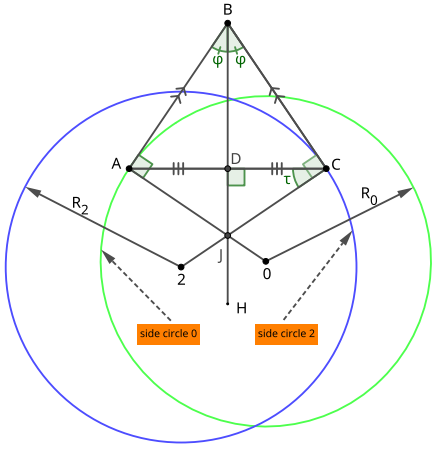

(d) **Type 3:** $|\overrightarrow{\mathbf{AB}}| = |\overrightarrow{\mathbf{BC}}|$ and $\overrightarrow{\mathbf{BH}} \times \overrightarrow{\mathbf{H0}} \geq 0$. R_0 = the radius of side circle 0, R_2 = the radius of side circle 2, BH is the bisector of ∠ABC, and $\overrightarrow{\mathbf{DJ}} \times \overrightarrow{\mathbf{J2}} < 0$. Side circle 0 and side circle 2 intersect each other.

Figure 5: **Type 3: $\mathbf{R_0}$ and $\mathbf{R_2}$ Construction**. R_0 and R_2 are defined for **Type 3** C-shaped triarcs in $\triangle ABC$.

Inequalities (10) and (11) ensure that side circle 0 intersects side circle 2, allowing for the successful construction of **Type 3** C-shaped triarcs. Thus, to construct a family of **Type 3** C-shaped triarcs, the approach coefficients α_0 and α_2 are introduced into the formulas for R_0 and R_2, respectively:

$$R_0 = \frac{\alpha_0 - 3}{3} \cdot |\overrightarrow{\mathbf{AB}}| \cdot \tan(\varphi), \quad (6 \le \alpha_0 < +\infty), \quad \text{where } \varphi \text{ is the half-angle of } \angle\text{ABC}. \tag{12a}$$

$$R_2 = \frac{\alpha_2 - 3}{3} \cdot \frac{|\overrightarrow{\mathbf{DC}}|}{\cos(\tau)}, \quad (6 < \alpha_2 < +\infty), \quad \text{where } \tau \text{ is } \angle\text{ACJ}. \tag{12b}$$

Eqs. (12a) and (12b) satisfy inequalities (10) and (11), respectively.

The process of constructing R_0 and R_2 is as follows: R_0 is calculated using Eq. (12a), and R_2 is calculated using Eq. (12b). Since R_0 and R_2 are independent of each other, the order of calculating R_0 and R_2 does not matter. The resulting R_0 and R_2 guarantee that $\overrightarrow{\mathbf{BH}} \times \overrightarrow{\mathbf{H0}} \ge 0$, side circle 0 intersects side circle 2, and point A lies inside side circle 2.

For the special case where $|\overrightarrow{\mathbf{AB}}| = |\overrightarrow{\mathbf{BC}}|$ (Fig. 5d), the same Eqs. (12a) and (12b) apply.

2.3 Construction of Radius $\mathbf{R_1}$ (Middle Circle 1)

As illustrated in Fig. 6, the middle circle 1 is tangent to side circles 0 and 2 at points 4 and 5, respectively, forming the triarc $\overset{\frown}{A45C}$. The triarc comprises three minor arcs: $\overset{\frown}{A4}$ and $\overset{\frown}{5C}$ (side arcs) and $\overset{\frown}{45}$ (middle arc).

The approach coefficient α_1 is introduced to serve as a shape control parameter defining R_1. Adjusting α_1 modifies R_1, thereby influencing the curvature and overall geometry of the C-shaped triarcs. The specific algebraic formulas of R_1 as functions of α_1 are presented in the following subsections for each triarc type.

R_1 is constructed such that increasing α_1 decreases R_1, which brings the triarc closer to vertex B; conversely, decreasing α_1 moves it farther away.

For the three types of C-shaped triarcs depicted in Fig. 6, α_1 is defined as:

- **Type 1 C-shaped triarc** (Fig. 6a): $-\infty < \alpha_1 \le 3$.
- **Type 2 C-shaped triarc** (Fig. 6b): $3 \le \alpha_1 \le 6$.
- **Type 3 C-shaped triarc** (Fig. 6c): $6 \le \alpha_1 < +\infty$.

To construct the C-shaped triarcs within $\triangle ABC$, the tangent points 4 and 5 must satisfy these inequalities:

$$\left.\begin{aligned} \overrightarrow{\mathbf{AC}} \times \overrightarrow{\mathbf{C4}} \ge 0 \\ \overrightarrow{\mathbf{CB}} \times \overrightarrow{\mathbf{B4}} \ge 0 \\ \overrightarrow{\mathbf{BA}} \times \overrightarrow{\mathbf{A4}} \ge 0 \end{aligned}\right\} \quad \text{for the tangent point 4 to lie inside } \triangle ABC. \tag{13}$$

$$\left.\begin{aligned} \overrightarrow{\mathbf{AC}} \times \overrightarrow{\mathbf{C5}} \ge 0 \\ \overrightarrow{\mathbf{CB}} \times \overrightarrow{\mathbf{B5}} \ge 0 \\ \overrightarrow{\mathbf{BA}} \times \overrightarrow{\mathbf{A5}} \ge 0 \end{aligned}\right\} \quad \text{for the tangent point 5 to lie inside } \triangle ABC. \tag{14}$$

Furthermore, the center 0 of side circle 0, the center 1 of middle circle 1, and the center 2 of side circle 2 should satisfy these inequalities:

$$\left.\begin{aligned} &\text{for } \textbf{Type 1}: \quad \overrightarrow{\mathbf{02}} \times \overrightarrow{\mathbf{21}} < 0 \\ &\text{for } \textbf{Type 2}: \quad \overrightarrow{\mathbf{02}} \times \overrightarrow{\mathbf{21}} > 0 \\ &\text{for } \textbf{Type 3}: \quad \overrightarrow{\mathbf{02}} \times \overrightarrow{\mathbf{21}} < 0 \end{aligned}\right\} \tag{15}$$

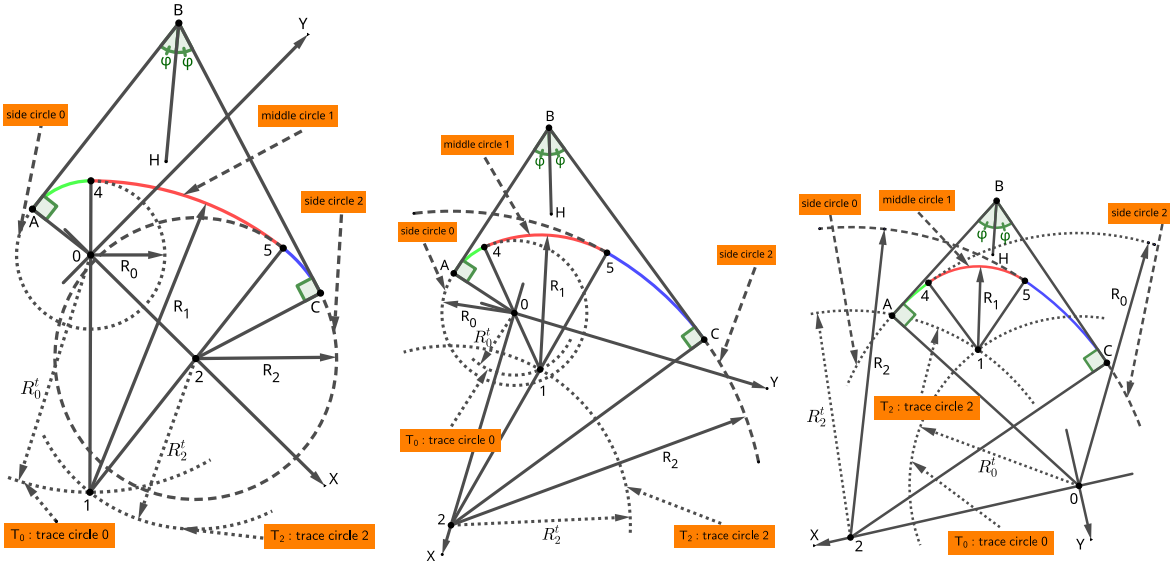

(a) **Type 1:** $|\overrightarrow{\mathbf{AB}}| < |\overrightarrow{\mathbf{BC}}|$. Both side circles 0 and 2 are internally tangent to middle circle 1 at the tangent points 4 and 5, respectively. $R_0^t = R_1 - R_0$; $R_2^t = R_1 - R_2$.

(b) **Type 2:** $|\overrightarrow{\mathbf{AB}}| < |\overrightarrow{\mathbf{BC}}|$. Side circle 0 is internally tangent to middle circle 1 at the tangent point 4, and middle circle 1 is internally tangent to side circle 2 at the tangent point 5. $R_0^t = R_1 - R_0$; $R_2^t = R_2 - R_1$.

(c) **Type 3:** $|\overrightarrow{\mathbf{AB}}| < |\overrightarrow{\mathbf{BC}}|$. Middle circle 1 is internally tangent to side circle 0 at the tangent point 4 and to side circle 2 at the tangent point 5. $R_0^t = R_0 - R_1$; $R_2^t = R_2 - R_1$.

Figure 6: **$\mathbf{R_1}$ Construction**. Side circle 0 is tangent to AB at point A and side circle 2 is tangent to BC at point C. Middle circle 1 is tangent to both side circles 0 and 2 at points 4 and 5, respectively. T_0 is the trace circle of side circle 0 and T_2 is the trace circle of side circle 2. R_0^t = the radius of trace circle T_0 and R_2^t = the radius of trace circle T_2. The triarc $\widehat{A45C}$ is composed of three minor circular arcs: $\widehat{A4}$, $\widehat{45}$, and $\widehat{5C}$ in which $\widehat{45}$ is the middle arc, and both $\widehat{A4}$ and $\widehat{5C}$ are the side arcs.

The boundary radius R_{4b} is defined as the specific value of R_1 where the tangent point 4 coincides with point A. Similarly, the boundary radius R_{5b} is defined as the specific value of R_1 where the tangent point 5 coincides with point C. These boundaries are crucial for ensuring the triarc is non-self-intersecting and lies within $\triangle ABC$. The detailed derivation and calculation of R_{4b} and R_{5b} are provided in Appendix A (Eqs. $A-11$ and $A-16$).

The supporting lemmas used in the following subsections are provided in Appendix B.

2.3.1 Construction of Radius $\mathbf{R_1}$ for Type 1 C-Shaped Triarcs (Fig. 6a)

R_{4b} and R_{5b} are the boundary radii of the middle circle 1 and can be calculated by Eqs. (A-11) and (A-16), respectively.

$$\text{Let } R_{45} = \max(R_{4b}, R_{5b}). \tag{16}$$

Actually, R_{45} can be simplified to $R_{45} = R_{5b}$ for the following two scenarios:

1. For $\triangle ABC$ with $|\overrightarrow{\mathbf{AB}}| < |\overrightarrow{\mathbf{BC}}|$, the tangent point 5 is outside $\triangle ABC$ when $R_1 = R_{4b}$; and both tangent points 4 and 5 are inside $\triangle ABC$ when $R_1 = R_{5b}$. Therefore, only R_{5b} is used for the construction of the formula R_1.

2. For an isosceles $\triangle ABC$ with $|\overrightarrow{\mathbf{AB}}| = |\overrightarrow{\mathbf{BC}}|$, have $R_{4b} = R_{5b}$.

It can be proven by **Lemmas** B.1 and B.4 that when $R_1 > R_{5b}$, the tangent points 4 and 5 lie inside $\triangle ABC$. Therefore, the equation for R_1 is constructed as:

$$R_1 = R_{5b} \cdot e^{(3-\alpha_1)(1.5\varphi+1)}, \quad (-\infty < \alpha_1 \leq 3), \quad \text{where } \varphi \text{ (in radians) is the half angle of } \angle \text{ABC}. \tag{17}$$

Proposition 1 of Eq. (17): If α_1 increases, R_1 decreases, and $R_1 \geq R_{5b}$ holds.
Proposition 2 of Eq. (17): For $R_{4b} \neq R_{5b}$ $\left(|\overrightarrow{\mathbf{AB}}| \neq |\overrightarrow{\mathbf{BC}}|\right)$, if $\alpha_1 = 3$, a triarc degenerates to a biarc.
Proposition 3 of Eq. (17): For $R_{4b} = R_{5b}$ $\left(|\overrightarrow{\mathbf{AB}}| = |\overrightarrow{\mathbf{BC}}|\right)$, if $\alpha_1 = 3$, a triarc degenerates to a single circular arc connecting points A and C.

From Eq. (17), have:

$$\lim_{\alpha_1 \to -\infty} R_1 = \lim_{\alpha_1 \to -\infty} R_{5b} \cdot e^{(3-\alpha_1)(1.5\varphi+1)} = +\infty.$$

Proposition 4 of Eq. (17): if $\alpha_1 \to -\infty$, have $R_1 \to +\infty$, meaning a middle circular arc degenerates to a straight-line segment.

2.3.2 Construction of Radius $\mathbf{R_1}$ for Type 2 C-Shaped Triarcs (Fig. 6b)

It can be proven that $R_{4b} < R_{5b}$ in $\triangle ABC$ with $|\overrightarrow{\mathbf{AB}}| < |\overrightarrow{\mathbf{BC}}|$. According to **Lemmas** B.2 and B.5, the tangent points 4 and 5 lie within $\triangle ABC$ when $R_{4b} < R_1 < R_{5b}$. Therefore, the equation for R_1 is given by:

$$R_1 = R_{5b} - \frac{(\alpha_1 - 3)(R_{5b} - R_{4b})}{3}, \quad (3 \leq \alpha_1 \leq 6). \tag{18}$$

Proposition 1 of Eq. (18): If α_1 increases, R_1 decreases within the interval $[R_{4b}, R_{5b}]$.
Proposition 2 of Eq. (18): When $\alpha_1 = 3$ and $|\overrightarrow{\mathbf{AB}}| \neq |\overrightarrow{\mathbf{BC}}|$, have $R_1 = R_{5b}$, meaning that a triarc degenerates to a biarc.
Proposition 3 of Eq. (18): When $\alpha_1 = 6$ and $|\overrightarrow{\mathbf{AB}}| \neq |\overrightarrow{\mathbf{BC}}|$, have $R_1 = R_{4b}$, meaning that a triarc degenerates to a biarc.
Proposition 4 of Eq. (18): When $|\overrightarrow{\mathbf{AB}}| = |\overrightarrow{\mathbf{BC}}|$, have $R_1 = R_{5b} = R_{4b}$, meaning that a triarc degenerates to a single circular arc with its radius being R_{5b}.

2.3.3 Construction of Radius $\mathbf{R_1}$ for Type 3 C-Shaped Triarcs (Fig. 6c)

Depending on the geometric relationship between point C and side circle 0, the boundary radius R_{5b} in Appendix A is invalid for the following two scenarios:

- If point C is outside side circle 0 or on the circumference of side circle 0, R_{5b} is invalid as the scenario of middle circle 1 being internally tangent to side circle 2 at point C and also internally tangent to side circle 0 does not exist.
- If point C is inside side circle 0, although R_{5b} can be calculated in Eq. (A-16), the corresponding tangent point 4 is outside $\triangle ABC$.

Instead, R_{4b} can be obtained directly from Eq. (A-11) without considering the relationship between point C and side circle 0.

Using **Lemmas** B.3 and B.6, it can be proven that when $R_1 < R_{4b}$, the tangent points 4 and 5 lie within $\triangle ABC$, regardless of whether point C is inside, outside, or on the circumference of side circle 0. Thus, the equation for R_1 is given by:

$$R_1 = R_{4b} \cdot e^{-\frac{\varphi(\alpha_1 - 6)}{14}}, \quad (6 \le \alpha_1 < +\infty), \\ \text{where } \varphi \text{ (in radians) is the half angle of } \angle \text{ABC}. \tag{19}$$

Proposition 1 of Eq. (19): If α_1 increases, then R_1 decreases, and $R_1 \le R_{4b}$ holds.
Proposition 2 of Eq. (19): When $\alpha_1 = 6$ and $|\overrightarrow{\mathbf{AB}}| \neq |\overrightarrow{\mathbf{BC}}|$, have $R_1 = R_{4b}$, meaning that a triarc degenerates to a biarc.
Proposition 3 of Eq. (19): When $\alpha_1 = 6$, $|\overrightarrow{\mathbf{AB}}| = |\overrightarrow{\mathbf{BC}}|$, point C is inside side circle 0, and point A is inside side circle 2, then the triarc degenerates to a single circular arc.

2.4 Summary of Radii Equations ($\mathbf{R_0}$, $\mathbf{R_1}$, $\mathbf{R_2}$)

For the three types of C-shaped triarcs in $\triangle ABC$, three approach coefficients (α_0, α_1, and α_2) are introduced to establish the equations for the radii R_0, R_1, and R_2, respectively. The functional relationships between the radii and their corresponding approach coefficients are as follows:

- R_0 is a strictly increasing function of α_0; thus, R_0 increases as α_0 increases and decreases as α_0 decreases. (Eqs. 3a, 6a, 9a, 12a)
- R_1 is a strictly decreasing function of α_1; thus, R_1 decreases as α_1 increases and increases as α_1 decreases. (Eqs. 17, 18, 19)
- R_2 is a strictly increasing function of α_2; thus, R_2 increases as α_2 increases and decreases as α_2 decreases. (Eqs. 3b, 6b, 9b, 12b)

The approach coefficients α_0, α_1, and α_2 serve as independent shape control parameters: increasing these coefficients moves the triarcs closer to the polyline ABC, while decreasing them moves the triarcs farther away.

While the current framework focuses on inflection-free C-shaped triarcs, the construction could, in principle, be extended to S-shaped (single-inflection) configurations. However, this study is intentionally restricted to convex C-shaped triarcs to guarantee predictable monotone approach behavior with respect to the control polyline. Introducing an inflection point would necessitate separate treatments for convex and concave segments, as well as additional constraints on the approach coefficients to ensure valid curve topologies. Consequently, extending the framework to S-shaped triarcs remains a subject for future research.

2.5 Algorithm for Triarc Construction

The algorithm assumes that the triangle ABC is non-degenerate. In practical implementations, numerical instabilities may occur in two degenerate scenarios: when the points are nearly collinear (the "flat" case) or when A and C reside on the same side of B (the "needle" case).

These configurations are detected by checking whether the magnitude of the cross product $\overrightarrow{\mathbf{BA}} \times \overrightarrow{\mathbf{BC}}$ falls below a prescribed tolerance ε. The dot product $P = \overrightarrow{\mathbf{BA}} \cdot \overrightarrow{\mathbf{BC}}$ is then used to distinguish between the flat ($P < 0$) and needle ($P > 0$) cases. As detailed in Step 2 of Algorithm 1, these cases are handled by approximating the curve with either a straight-line segment or a fractional polyline to ensure numerical and geometric robustness.

Algorithm 1 Algorithm for constructing a C-shaped triarc within $\triangle ABC$ from the approach coefficients.

Input: Points A, B, C; triarc type $T \in \{1,2,3\}$; approach coefficients $\alpha_0, \alpha_1, \alpha_2$; tolerance ε.
Output: Centers O_0, O_1, O_2; radii R_0, R_1, R_2; tangent points P_4, P_5.

1: **Pre-processing:** Construct the control polyline ABC. Without loss of generality, assume $\overrightarrow{\mathbf{BA}} \times \overrightarrow{\mathbf{BC}} < 0$ (CW orientation) and $|\overrightarrow{\mathbf{AB}}| \le |\overrightarrow{\mathbf{BC}}|$, applying a coordinate transformation if necessary;
2: **Check for Degenerate Geometry:**
If $|\overrightarrow{\mathbf{BA}} \times \overrightarrow{\mathbf{BC}}| < \varepsilon$ **and** $\overrightarrow{\mathbf{BA}} \cdot \overrightarrow{\mathbf{BC}} < 0$ (nearly flat), **then** approximate with linear segment AC and terminate;
Else if $|\overrightarrow{\mathbf{BA}} \times \overrightarrow{\mathbf{BC}}| < \varepsilon$ **and** $\overrightarrow{\mathbf{BA}} \cdot \overrightarrow{\mathbf{BC}} > 0$ (nearly needle):
- **If** $T \in \{1,2\}$, **then** approximate with linear segment AC and terminate;
- **If** $T = 3$, **then** approximate with a fractional polyline ABC where the length is proportional to $\max(\alpha_0, \alpha_1, \alpha_2)$ and terminate;

3: Compute $R_0 \leftarrow f_0(\alpha_0)$ and $R_2 \leftarrow f_2(\alpha_2, [R_0, T])$ using the formulas in Section 2.2, evaluating R_0 first;
4: Compute the side arc centers O_0 and O_2;
5: Compute the boundary radii R_{4b} and R_{5b} (Eqs. A-11 and A-16);
6: **If** the approach coefficients correspond to boundary cases (Inequalities A-8 or A-13), **then** construct the corresponding biarc and terminate the algorithm;
7: Compute $R_1 \leftarrow f_1(\alpha_1)$ using the formulas in Section 2.3;
8: Compute the middle arc center $O_1 = (X_1, Y_1)$ (Eqs. A-2a and A-2b);
9: Compute the tangent points $P_4 = (X_4, Y_4)$ (Eqs. A-4a and A-4b) and $P_5 = (X_5, Y_5)$ (Eqs. A-6a and A-6b);
10: **Output** the resulting triarc with centers $O_{0,1,2}$, radii $R_{0,1,2}$, and tangent points $P_{4,5}$.

3 APPROACH THEOREMS FOR TYPE 1, TYPE 2, and TYPE 3 C-SHAPED TRIARCS

Three factors, R_0, R_1, and R_2, contribute to the construction of C-shaped triarcs that possess approach and anti-approach properties, which warrant further discussion.

3.1 Definitions

The approach ratio quantifies the proximity between a curve segment and the reference polyline ABC within $\triangle ABC$ and applies to all subsequent approach definitions. It is defined as:

$$\xi = \frac{\text{Area enclosed by AB, BC, and the curve segment from A to C}}{\text{Area of } \triangle ABC}, \quad (0 \le \xi \le 1). \tag{20}$$

Definition 3.1.1 (**General and Anti-general Approaches**). (Fig. 7) Let C_1 and C_2 be two curve segments within $\triangle ABC$, each extending from point A to point C. **General Approach** (resp. **Anti-general Approach**) is defined as the case where the curve segment C_2 is closer to (resp. farther from) the polyline ABC than C_1 if the area enclosed by C_2 and the polyline ABC is smaller (resp. greater) than the area enclosed by C_1 and the polyline ABC.

Only the enclosed area is considered for both **General Approach** and **Anti-general Approach** concepts. Therefore, C_1 and C_2 may intersect each other.

Definition 3.1.2 (**Strict and Anti-strict Approaches**). (Fig. 8) Let C_1 and C_2 be two curve segments within $\triangle ABC$, each extending from point A to point C. Both C_1 and C_2 are non-self-intersecting and have no inflection points. Let any ray $\mathscr{R}$ originating from vertex B pass through any point on the straight-line segment AC (excluding endpoints A and C). Two intersection points, A_1 and A_2, are generated between $\mathscr{R}$ and the two curve segments, C_1 and C_2, respectively.

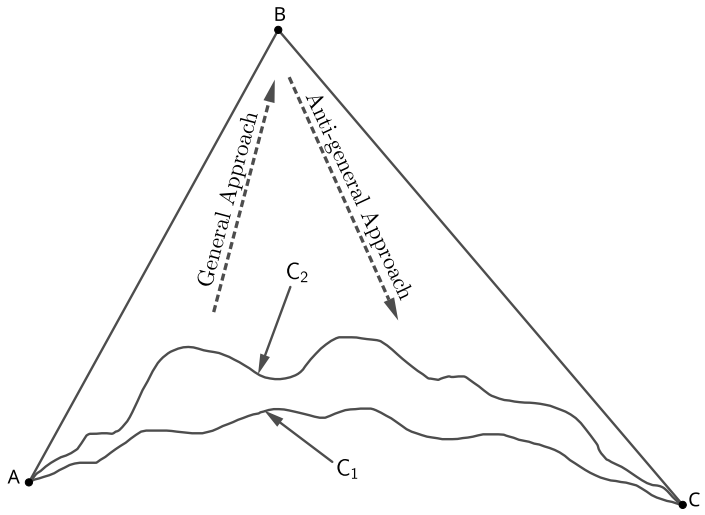

Figure 7: **General Approach:** C_2 approaches the polyline ABC more closely than C_1 with $\xi_2 < \xi_1$. **Anti-general Approach:** C_1 moves farther away from the polyline ABC than C_2 with $\xi_1 > \xi_2$.

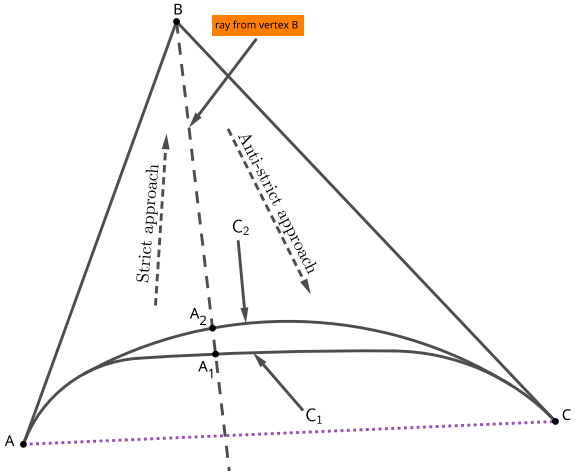

Figure 8: **Strict Approach:** C_2 strictly approaches the polyline ABC more closely than C_1. **Anti-strict Approach:** C_1 strictly recedes from the polyline ABC farther than C_2. C_1 and C_2 overlap partially.

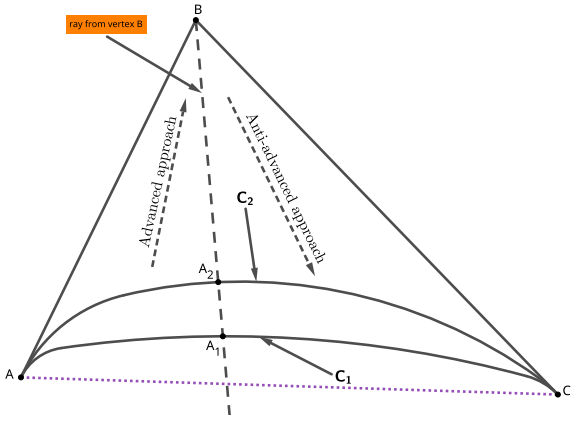

Figure 9: **Advanced Approach:** C_2 completely approaches the polyline ABC more closely than C_1. **Anti-advanced Approach:** C_1 completely moves farther away from the polyline ABC than C_2. C_1 and C_2 do not overlap.

Strict Approach (resp. **Anti-strict Approach**) is defined as the case where C_2 approaches (resp. recedes from) the polyline ABC relative to C_1 if the following conditions hold:

1. For all rays $\mathscr{R}$ from vertex B intersecting AC (excluding A and C), the distance from A_2 to B is less than or equal to (resp. greater than or equal to) the distance from A_1 to B, i.e.,

$$|\overrightarrow{\mathbf{A_2B}}| \leq |\overrightarrow{\mathbf{A_1B}}| \quad \text{(resp. } |\overrightarrow{\mathbf{A_2B}}| \geq |\overrightarrow{\mathbf{A_1B}}|\text{)}.$$

2. There exists at least one ray $\mathscr{R}$ such that the distance from A_2 to B is strictly less than (resp. greater than) the distance from A_1 to B, i.e.,

$$|\overrightarrow{\mathbf{A_2B}}| < |\overrightarrow{\mathbf{A_1B}}| \quad (\text{resp. } |\overrightarrow{\mathbf{A_2B}}| > |\overrightarrow{\mathbf{A_1B}}|).$$

3. There exists at least one ray $\mathscr{R}$ such that A_1 and A_2 coincide, i.e., $\overrightarrow{\mathbf{A_1}} = \overrightarrow{\mathbf{A_2}}$.

Definition 3.1.3 (**Advanced and Anti-advanced Approaches**). (Fig. 9) Let C_1 and C_2 be two curve segments within $\triangle ABC$, each extending from point A to point C. Both C_1 and C_2 are non-self-intersecting and have no inflection points. Let any ray $\mathscr{R}$ originating from vertex B pass through any point on the straight-line segment AC (excluding endpoints A and C). Two intersection points, A_1 and A_2, are generated between $\mathscr{R}$ and the two curve segments, C_1 and C_2, respectively.

Advanced Approach is defined as the case where C_2 completely approaches the polyline ABC more closely than C_1, that is, on every $\mathscr{R}$, the point A_2 lies closer to vertex B than A_1, meaning $|\overrightarrow{\mathbf{A_2B}}| < |\overrightarrow{\mathbf{A_1B}}|$ is always true.

Conversely, **Anti-advanced Approach** is defined as the case where C_1 completely moves farther away from the polyline ABC than C_2, that is, on every $\mathscr{R}$, the point A_1 lies farther from vertex B than A_2, meaning $|\overrightarrow{\mathbf{A_1B}}| > |\overrightarrow{\mathbf{A_2B}}|$ is always true.

The difference between advanced approach and strict approach or between anti-advanced approach and anti-strict approach is that the two curve segments, C_1 and C_2, never overlap in advanced approach and in anti-advanced approach; however, they overlap in strict approach and in anti-strict approach.

3.2 One-Factor Strict Approach Theorems and Proofs by Varying $\mathbf{R_0}$, $\mathbf{R_1}$, or $\mathbf{R_2}$

Strict approach can be accomplished by changing only one factor R_0, R_1, or R_2.

Notation 1 (Triarc Analysis). *All figures and equations in this section (Figs. 10–18) share the same geometric conventions.*

General conventions. *Superscripts* 1 *and* 2 *denote two distinct states or configurations of a quantity (e.g., initial state 1 and modified state 2), not powers. The superscript* 3 *is used separately to denote specific derived intersection points, as defined below. Each state (1 or 2) thus forms a C-shaped triarc within $\triangle ABC$, where side circles 0 and 2 are tangent to edges AB and BC at points A and C, respectively, and the middle circle 1 is tangent to both side circles 0 and 2.*

- R_0, R_1, R_2 *– radii of side circle 0, middle circle 1, and side circle 2, respectively.*
- R_i^1, R_i^2 *– initial and modified radii of circle i; ΔR_i – radius change, defined as $\Delta R_i = R_i^2 - R_i^1$ for side circles ($i = 0, 2$), and $\Delta R_1 = R_1^1 - R_1^2$ for middle circle.*
- T_i, T_i^1, T_i^2 *– trace circles associated with side circle i ($i = 0, 2$); R_i^t, R_i^{t1}, and R_i^{t2} – their respective radii, defined as $R_i^t = |R_1 - R_i|$, $R_i^{t1} = |R_1^1 - R_i|$ (Figs. 10–12) or $|R_1 - R_i^1|$ (Figs. 13–18), and $R_i^{t2} = |R_1^2 - R_i|$ (Figs. 10–12) or $|R_1 - R_i^2|$ (Figs. 13–18) ($i = 0, 2$).*
- C_1, C_2 *– triarcs before and after the radius modification. Two triarcs are defined in each figure:*
  - ***Varying*** R_1***:*** *circles* 0 *and* 2 *are fixed; circles* 1^1 *and* 1^2 *define triarcs C_1 and C_2.*
  - ***Varying*** R_0***:*** *circles* 1 *and* 2 *are fixed; circles* 0^1 *and* 0^2 *define triarcs C_1 and C_2.*
  - ***Varying*** R_2***:*** *circles* 0 *and* 1 *are fixed; circles* 2^1 *and* 2^2 *define triarcs C_1 and C_2.*
- *Points A_4^j and A_5^j – tangent points between the middle circle and the two side circles ($j = 1$ for C_1 and $j = 2$ for C_2). Points A_4^3 and A_5^3 – intersection points between the middle circular arcs of C_1 and/or C_2 and the straight lines through the centers 1^1 and/or 1^2 of the middle circles.*

- ξ – *approach ratio (Eq. 20), measuring the area-based proximity of a triarc to its control polyline ABC.*

All theorems, proofs, and figures in Section 3.2 follow this unified notation.

3.2.1 Strict Approach Theorem for Varying One Factor $\mathbf{R_1}$

Theorem 3.1 (One-Factor Strict Approach Theorem by Varying R_1)**.** For a C-shaped triarc of **Type 1** (Fig. 10), **Type 2** (Fig. 11), or **Type 3** (Fig. 12) constructed within $\triangle ABC$, subject to the appropriate edge-length conditions:

- $|\overrightarrow{\mathbf{AB}}| \leq |\overrightarrow{\mathbf{BC}}|$ (for **Type 1** and **Type 3**).
- $|\overrightarrow{\mathbf{AB}}| < |\overrightarrow{\mathbf{BC}}|$ (for **Type 2**).

given that the side circular arc radii R_0 and R_2 are fixed:

1. When the middle circular arc radius R_1 decreases, the triarc must strictly approach its control polyline ABC.
2. When the middle circular arc radius R_1 increases, the triarc must strictly anti-approach its control polyline ABC.

This theorem can be proven separately for the three types of C-shaped triarcs. All supporting lemmas for this section are provided in Appendix B.

3.2.1.1 Proof for Type 1 by Varying One Factor $\mathbf{R_1}$

*Proof for **Type 1** Triarcs (Fig. 10).* Suppose that the middle circle 1^1 with the radius R_1^1 is tangent to side circles 0 and 2 at points A_4^1 and A_5^1, respectively. When R_1 decreases from R_1^1 to R_1^2 by $\triangle R_1$, the resulting middle circle 1^2 with the radius R_1^2 is tangent to side circles 0 and 2 at points A_4^2 and A_5^2, respectively. After R_1 decreases from R_1^1 to R_1^2, according to **Lemma** B.1, X_4 decreases, indicating that A_4^1 moves negatively to A_4^2 on the circumference of side circle 0 along the X-axis; according to **Lemma** B.4, X_5 increases, indicating that A_5^1 moves positively to A_5^2 on the circumference of side circle 2 along the X-axis. Let the straight line $1^10A_4^1$ intersect the middle circle 1^2 at point A_4^3, and let $1^12A_5^1$ intersect the middle circle 1^2 at point A_5^3. It is proven that both A_4^3 and A_5^3 lie outside the middle circle 1^1. Therefore, the triarc $C_2\left(\widehat{AA_4^2A_4^3A_5^3A_5^2C}\right)$ strictly approaches the polyline ABC more closely than the triarc $C_1\left(\widehat{AA_4^2A_4^1A_5^1A_5^2C}\right)$ although there are overlapping segments $\widehat{AA_4^2}$ and $\widehat{A_5^2C}$. Consequently, strict approach must occur when R_1 decreases from R_1^1 to R_1^2 given that both R_0 and R_2 are fixed.

Conversely, suppose that R_1 increases from R_1^2 to R_1^1 (where $R_1^1 > R_1^2$) by $\triangle R_1$. By reversing the logic based on **Lemma** B.1 and **Lemma** B.4, X_4 increases and X_5 decreases, indicating that A_4^2 moves positively to A_4^1 and A_5^2 moves negatively to A_5^1. Constructing analogous intersection points shows that C_1 is further away from the control polyline ABC compared to C_2. Therefore, anti-strict approach must occur when R_1 increases, given fixed R_0 and R_2. □

If $|\overrightarrow{\mathbf{AB}}| < |\overrightarrow{\mathbf{BC}}|$, the approaching ratio ξ decreases when R_1 decreases. The triarc C_2 degenerates to a biarc when A_5^2 coincides with point C after R_1 decreases sufficiently.

If $|\overrightarrow{\mathbf{AB}}| = |\overrightarrow{\mathbf{BC}}|$, the triarc C_2 degenerates to a single circular arc connecting points A and C when A_5^2 coincides with point C after R_1 decreases sufficiently.

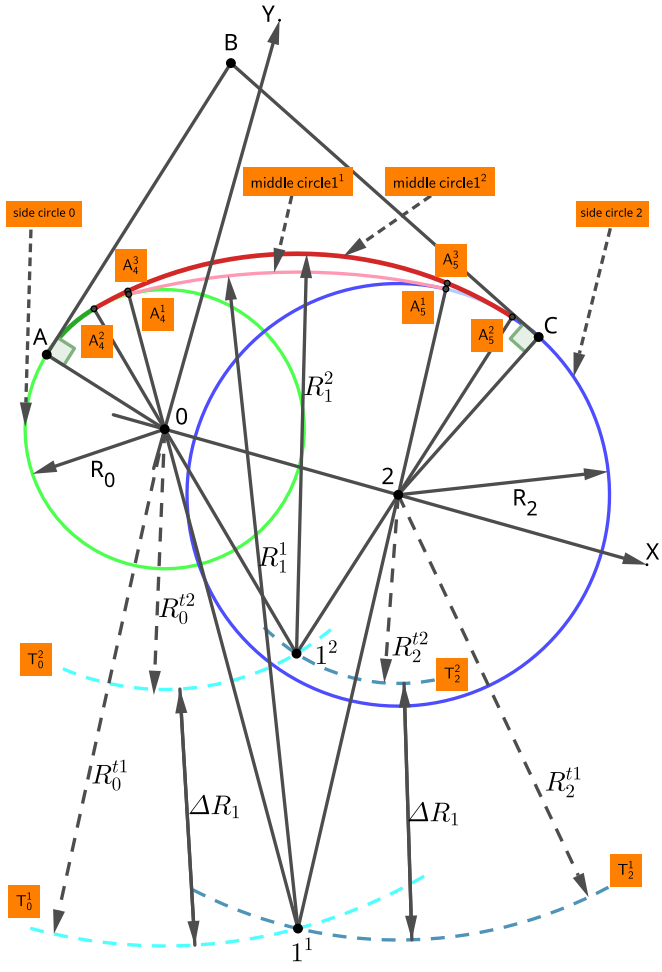

Figure 10: **Type 1 Strict Approach for R_1 ↘. $|\overrightarrow{AB}| \le |\overrightarrow{BC}|$.** Both side circles 0 and 2 are internally tangent to the middle circles 1^1 and 1^2. The middle circle 1^1 is tangent to side circles 0 and 2 at points A_4^1 and A_5^1, respectively; the middle circle 1^2 is tangent to side circles 0 and 2 at points A_4^2 and A_5^2, respectively. The triarc $C_2\left(\widehat{AA_4^2A_4^3A_5^3A_5^2C}\right) = \widehat{AA_4^2}$ (side circular arc) + $\widehat{A_4^2A_4^3A_5^3A_5^2}$ (middle circular arc) + $\widehat{A_5^2C}$ (side circular arc); the triarc $C_1\left(\widehat{AA_4^2A_4^1A_5^1A_5^2C}\right) = \widehat{AA_4^2A_4^1}$ (side circular arc) + $\widehat{A_4^1A_5^1}$ (middle circular arc) + $\widehat{A_5^1A_5^2C}$ (side circular arc). C_2 strictly approaches the polyline ABC more closely than C_1 when R_1 decreases from R_1^1 to R_1^2 given that both R_0 and R_2 are fixed. Notation follows Notation1.

3.2.1.2 Proof for Type 2 by Varying One Factor R_1

*Proof for **Type 2** Triarcs (Fig. 11).* Suppose that the middle circle 1^1 with the radius R_1^1 is tangent to side circles 0 and 2 at points A_4^1 and A_5^1, respectively. When R_1 decreases from R_1^1 to R_1^2 by $\triangle R_1$, the resulting middle circle 1^2 with the radius R_1^2 is tangent to side circles 0 and 2 at points A_4^2 and A_5^2, respectively. After R_1 decreases from R_1^1 to R_1^2, according to **Lemma** B.2, X_4 increases, indicating that A_4^1 moves positively to A_4^2 on the circumference of side circle 0 along the X-axis; according to **Lemma** B.5, X_5 decreases, indicating

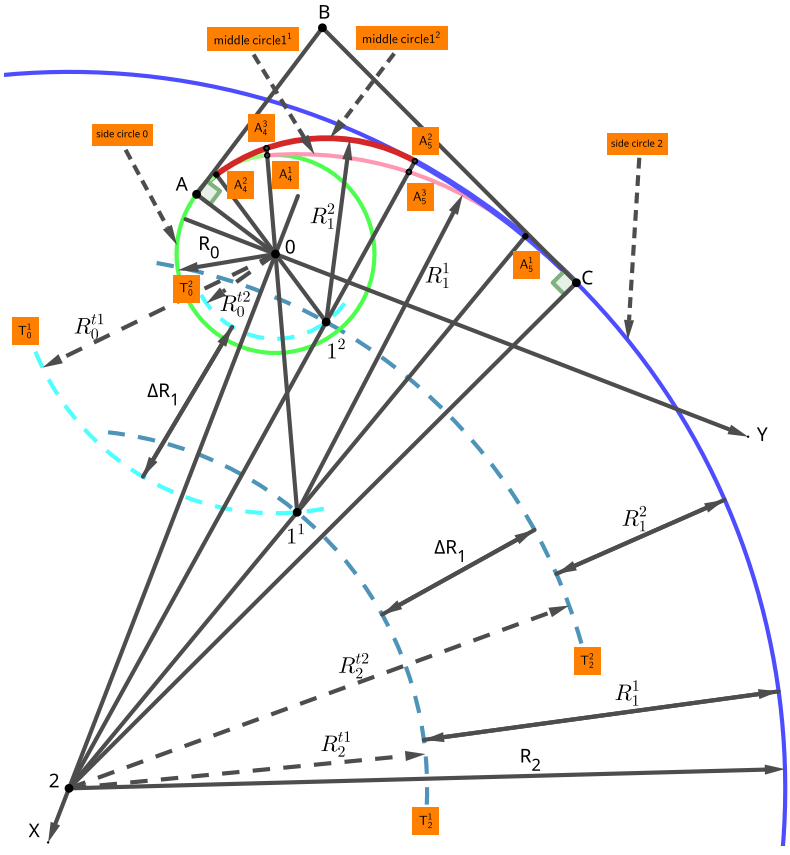

Figure 11: **Type 2 Strict Approach for R_1 ↘. $|\overrightarrow{\mathbf{AB}}| < |\overrightarrow{\mathbf{BC}}|$.** Side circle 0 is internally tangent to the middle circles 1^1 and 1^2 that are internally tangent to side circle 2. The middle circle 1^1 is tangent to side circles 0 and 2 at points A_4^1 and A_5^1, respectively; the middle circle 1^2 is tangent to side circles 0 and 2 at points A_4^2 and A_5^2, respectively. The triarc $C_2\left(\widehat{AA_4^2A_4^3A_5^2A_5^1C}\right) = \widehat{AA_4^2}$ (side circular arc) + $\widehat{A_4^2A_4^3A_5^2}$ (middle circular arc) + $\widehat{A_5^2A_5^1C}$ (side circular arc); the triarc $C_1\left(\widehat{AA_4^2A_4^1A_5^3A_5^1C}\right) = \widehat{AA_4^2A_4^1}$ (side circular arc) + $\widehat{A_4^1A_5^3A_5^1}$ (middle circular arc) + $\widehat{A_5^1C}$ (side circular arc). C_2 strictly approaches the polyline ABC more closely than C_1 when R_1 decreases from R_1^1 to R_1^2 given that both R_0 and R_2 are fixed. Notation follows Notation1.

that A_5^1 moves negatively to A_5^2 on the circumference of side circle 2 along the X-axis. Let the straight line $1^10A_4^1$ intersect the middle circle 1^2 at point A_4^3, and let $21^2A_5^2$ intersect the middle circle 1^1 at point A_5^3. It is proven that both A_4^3 and A_5^2 lie outside the middle circle 1^1. Therefore, the triarc $C_2\left(\widehat{AA_4^2A_4^3A_5^2A_5^1C}\right)$ strictly approaches the polyline ABC more closely than $C_1\left(\widehat{AA_4^2A_4^1A_5^3A_5^1C}\right)$ although there are overlapping segments $\widehat{AA_4^2}$ and $\widehat{A_5^1C}$. Consequently, strict approach must occur when R_1 decreases from R_1^1 to R_1^2 given that both R_0 and R_2 are fixed.

Conversely, increasing R_1 causes the tangent points to move in opposite directions compared to the decreasing case, resulting in the triarc strictly anti-approaching the control polyline ABC. □

If $|\overrightarrow{\mathbf{AB}}| < |\overrightarrow{\mathbf{BC}}|$, the triarc C_2 degenerates to a biarc when A_4^2 coincides with point A after R_1 decreases sufficiently or when A_5^2 coincides with point C after R_1 increases sufficiently.

If $|\overrightarrow{\mathbf{AB}}| = |\overrightarrow{\mathbf{BC}}|$, a triarc degenerates to a single circular arc connecting points A and C.

3.2.1.3 Proof for Type 3 by Varying One Factor $\mathbf{R_1}$

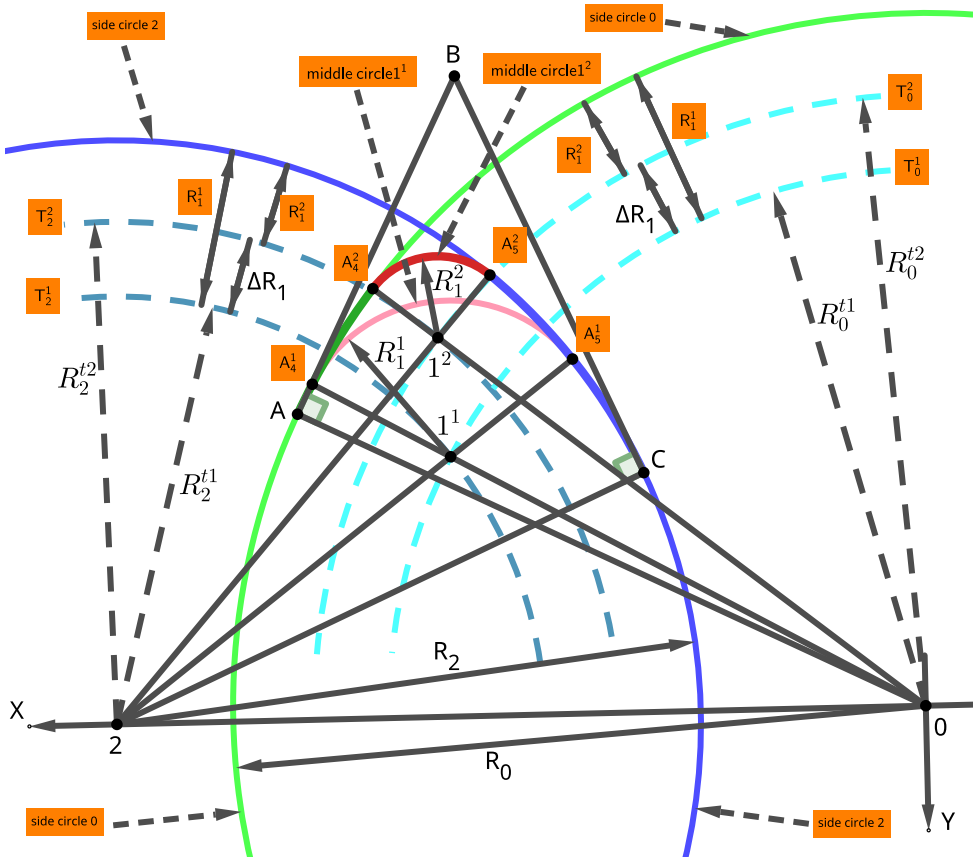

Figure 12: **Type 3 Strict Approach for $R_1 \searrow$. $|\overrightarrow{\mathbf{AB}}| \le |\overrightarrow{\mathbf{BC}}|$.** The middle circle 1^1 is internally tangent to side circles 0 and 2 at points A_4^1 and A_5^1, respectively; the middle circle 1^2 is internally tangent to side circles 0 and 2 at points A_4^2 and A_5^2, respectively. The triarc $C_2\left(\widehat{AA_4^1A_4^2A_5^2A_5^1C}\right) = \widehat{AA_4^1A_4^2}$ (side circular arc) + $\widehat{A_4^2A_5^2}$ (middle circular arc) + $\widehat{A_5^2A_5^1C}$ (side circular arc); the triarc $C_1\left(\widehat{AA_4^1A_5^1C}\right) = \widehat{AA_4^1}$ (side circular arc) + $\widehat{A_4^1A_5^1}$ (middle circular arc) + $\widehat{A_5^1C}$ (side circular arc). C_2 strictly approaches the polyline ABC more closely than C_1 when R_1 decreases from R_1^1 to R_1^2 given that both R_0 and R_2 are fixed. Notation follows Notation1.

Proof for ***Type 3*** *Triarcs (Fig. 12).* Suppose that the middle circle 1^1 with the radius R_1^1 is tangent to side circles 0 and 2 at points A_4^1 and A_5^1, respectively. When R_1 decreases from R_1^1 to R_1^2 by $\triangle R_1$, the resulting middle circle 1^2 with the radius R_1^2 is tangent to side circles 0 and 2 at points A_4^2 and A_5^2, respectively. After R_1 decreases from R_1^1 to R_1^2, according to **Lemma** B.3, X_4 decreases, indicating that A_4^1 moves negatively to

A_4^2 on the circumference of side circle 0 along the X-axis; according to **Lemma** B.6, X_5 increases, indicating that A_5^1 moves positively to A_5^2 on the circumference of side circle 2 along the X-axis. It is proven that both A_4^2 and A_5^2 lie outside the middle circle 1^1. Because the curvature of middle circle 1^2 is larger than that of middle circle 1^1 due to $R_1^2 < R_1^1$, the middle circular arc $\overset{\frown}{A_4^2A_5^2}$ lies entirely outside the middle circle 1^1. Therefore, the triarc $C_2\left(\overset{\frown}{AA_4^1A_4^2A_5^2A_5^1C}\right)$ strictly approaches the polyline ABC more closely than $C_1\left(\overset{\frown}{AA_4^1A_5^1C}\right)$ although there are overlapping segments $\overset{\frown}{AA_4^1}$ and $\overset{\frown}{A_5^1C}$. Consequently, strict approach must occur when R_1 decreases from R_1^1 to R_1^2 given that both R_0 and R_2 are fixed.

Conversely, increasing R_1 causes the tangent points to move in opposite directions compared to the decreasing case, resulting in the triarc strictly anti-approaching the control polyline ABC. □

If $|\overrightarrow{\mathbf{AB}}| < |\overrightarrow{\mathbf{BC}}|$, the triarc C_1 degenerates to a biarc when A_4^1 coincides with point A after R_1 increases sufficiently.

If $|\overrightarrow{\mathbf{AB}}| = |\overrightarrow{\mathbf{BC}}|$, point C is inside the circle 0, and point A is inside the circle 2, the triarc C_1 degenerates to a single circular arc connecting points A and C when A_4^1 coincides with point A or A_4^2 coincides with point C after R_1 increases sufficiently.

3.2.2 Strict Approach Theorem for Varying One Factor $\mathbf{R_0}$

Theorem 3.2 (One-Factor Strict Approach Theorem by Varying R_0)**.** For a C-shaped triarc of **Type 1** (Fig. 13), **Type 2** (Fig. 14), or **Type 3** (Fig. 15) constructed within $\triangle ABC$, subject to the appropriate edge-length conditions:

- $|\overrightarrow{\mathbf{AB}}| \le |\overrightarrow{\mathbf{BC}}|$ (for **Type 1** and **Type 3**).
- $|\overrightarrow{\mathbf{AB}}| < |\overrightarrow{\mathbf{BC}}|$ (for **Type 2**).

given that the middle circular arc radius R_1 and the side circular arc radius R_2 are fixed:

1. When the side circular arc radius R_0 increases, the triarc must strictly approach its control polyline ABC.
2. When the side circular arc radius R_0 decreases, the triarc must strictly anti-approach its control polyline ABC.

This theorem can be proven separately for the three types of C-shaped triarcs.

3.2.2.1 Proof for Type 1 by Varying One Factor $\mathbf{R_0}$

*Proof for **Type 1** Triarcs (Fig. 13).* Suppose that the middle circle 1^1 with the radius R_1 is tangent to side circles 0^1 and 2 at points A_4^1 and A_5^1, respectively; the middle circle 1^2 with the same radius R_1 is tangent to side circles 0^2 and 2 at points A_4^2 and A_5^2, respectively. When R_0 increases from R_0^1 to R_0^2 by $\triangle R_0$, have $|\overrightarrow{\mathbf{0^1 0^2}}| + |\overrightarrow{\mathbf{0^2 1^2}}| > |\overrightarrow{\mathbf{0^1 1^1}}|$. In order to keep R_1 fixed and to remain the center 1^2 of the middle circle 1^2 to be on the trace circle T_2, have $|\overrightarrow{\mathbf{0^2 1^2}}| < |\overrightarrow{\mathbf{0^2 1^1}}|$ as $R_0^2 > R_0^1$, $R_0^2 + |\overrightarrow{\mathbf{0^2 1^2}}| = R_1$, and $R_0^2 + |\overrightarrow{\mathbf{0^2 1^1}}| > R_1$. Therefore, 1^2 is obtained by rotating 1^1 clockwise around the center (point 2) of trace circle T_2 by an angle θ along T_2. As a result, A_5^2 is obtained by rotating A_5^1 clockwise around the center (point 2) of side circle 2 by an angle θ on the circumference of side circle 2. Obviously, point A_4^2 lies outside the middle circle 1^1 and the circular arc $\overset{\frown}{A_4^2A_5^2}$ lies outside the biarc $\overset{\frown}{A_4^1A_5^1A_5^2}$ $\left(\overset{\frown}{A_4^1A_5^1} + \overset{\frown}{A_5^1A_5^2}\right)$. Therefore, the triarc $C_2\left(\overset{\frown}{AA_4^2A_5^2C}\right)$ strictly approaches the polyline ABC more closely than $C_1\left(\overset{\frown}{AA_4^1A_5^1A_5^2C}\right)$ although there is an overlapping segment: $\overset{\frown}{A_5^2C}$. Consequently, strict approach must occur when R_0 increases from R_0^1 to R_0^2 given that both R_1 and R_2 are fixed.

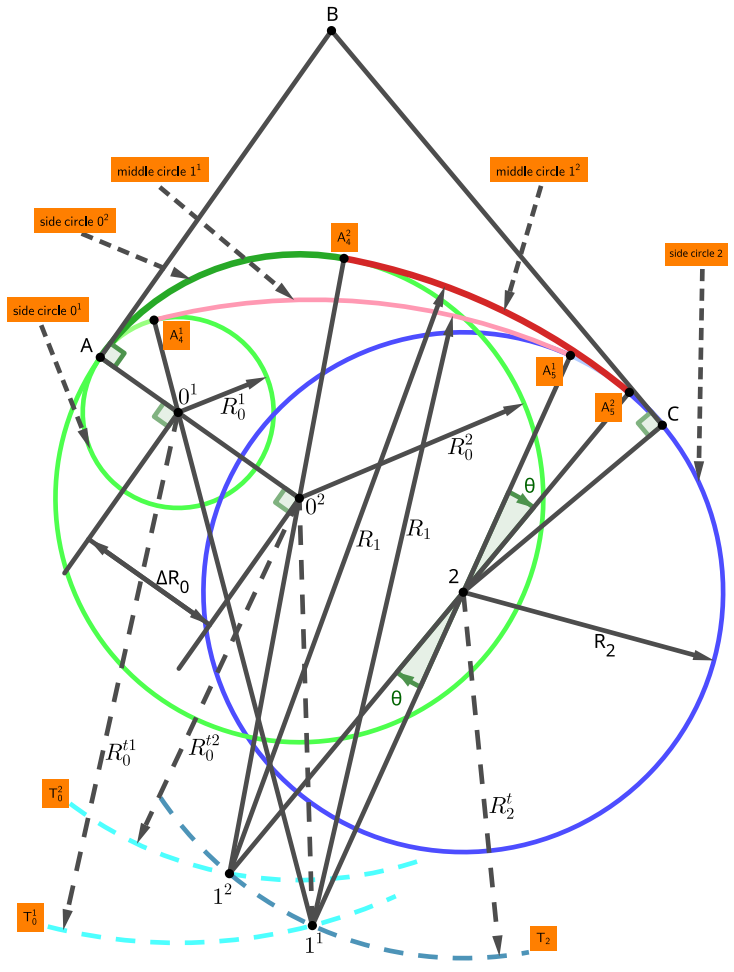

Figure 13: **Type 1 Strict Approach for R_0 ↗.** $|\overrightarrow{\mathbf{AB}}| \leq |\overrightarrow{\mathbf{BC}}|$. Side circles 0^1 and 2 are internally tangent to the middle circle 1^1 at points A_4^1 and A_5^1, respectively; side circles 0^2 and 2 are internally tangent to the middle circle 1^2 at points A_4^2 and A_5^2, respectively. The triarc $C_2\left(\widehat{AA_4^2A_5^2C}\right)$ = $\widehat{AA_4^2}$ (side circular arc) + $\widehat{A_4^2A_5^2}$ (middle circular arc) + $\widehat{A_5^2C}$ (side circular arc); the triarc $C_1\left(\widehat{AA_4^1A_5^1A_5^2C}\right)$ = $\widehat{AA_4^1}$ (side circular arc) + $\widehat{A_4^1A_5^1}$ (middle circular arc) + $\widehat{A_5^1A_5^2C}$ (side circular arc). C_2 strictly approaches the polyline ABC more closely than C_1 when R_0 increases from R_0^1 to R_0^2 given that both R_1 and R_2 are fixed. Notation follows Notation1.

Conversely, reducing R_0 from R_0^2 to R_0^1 causes the triarc C_2 to move away from the control polyline ABC, leading to an anti-strict approach. □

3.2.2.2 Proof for Type 2 by Varying One Factor $\mathbf{R_0}$

*Proof for **Type 2** Triarcs (Fig. 14).* Suppose that the middle circle 1^1 with the radius R_1 is tangent to side circles 0^1 and 2 at points A_4^1 and A_5^1, respectively; the middle circle 1^2 with the radius R_1 is tangent to

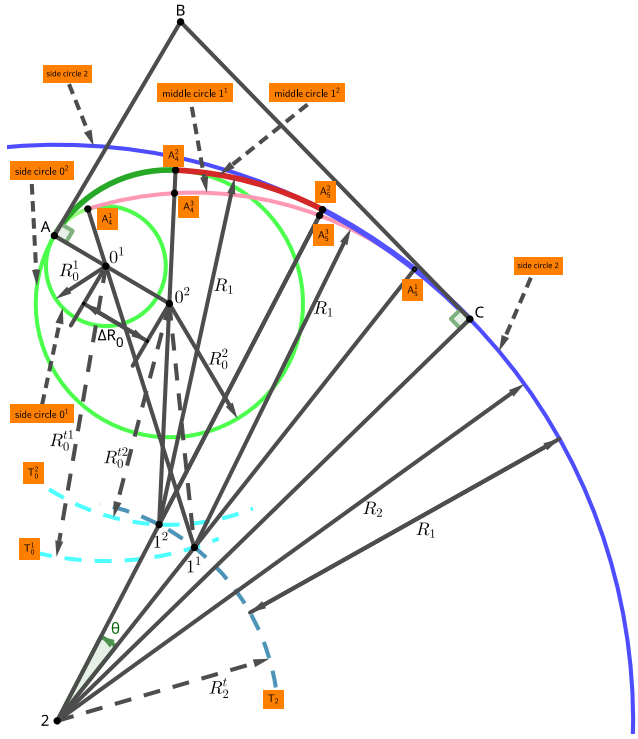

Figure 14: **Type 2 Strict Approach for R_0 ↗. $|\overrightarrow{\mathbf{AB}}| < |\overrightarrow{\mathbf{BC}}|$.** Side circle 0^1 is internally tangent to the middle circle 1^1 that is internally tangent to side circle 2; side circle 0^2 is internally tangent to the middle circle 1^2 that is internally tangent to side circle 2. The middle circle 1^1 is tangent to side circles 0^1 and 2 at points A_4^1 and A_5^1, respectively; the middle circle 1^2 is tangent to side circles 0^2 and 2 at points A_4^2 and A_5^2, respectively. The triarc $C_2\left(\widehat{AA_4^2A_5^2A_5^1C}\right) = \widehat{AA_4^2}$ (side circular arc) + $\widehat{A_4^2A_5^2}$ (middle circular arc) + $\widehat{A_5^2A_5^1C}$ (side circular arc); the triarc $C_1\left(\widehat{AA_4^1A_4^3A_5^3A_5^1C}\right) = \widehat{AA_4^1}$ (side circular arc) + $\widehat{A_4^1A_4^3A_5^3A_5^1}$ (middle circular arc) + $\widehat{A_5^1C}$ (side circular arc). C_2 strictly approaches the polyline ABC more closely than C_1 when R_0 increases from R_0^1 to R_0^2 given that both R_1 and R_2 are fixed. Notation follows Notation1.

side circles 0^2 and 2 at points A_4^2 and A_5^2, respectively. When R_0 increases from R_0^1 to R_0^2 by $\triangle R_0$, have $|\overrightarrow{\mathbf{0^1 0^2}}| + |\overrightarrow{\mathbf{0^2 1^1}}| > |\overrightarrow{\mathbf{0^1 1^1}}|$. In order to keep R_1 fixed and to remain the center (point 1^2) of the middle circle 1^2 to be on the trace circle T_2, have $|\overrightarrow{\mathbf{0^2 1^2}}| < |\overrightarrow{\mathbf{0^2 1^1}}|$ as $R_0^2 > R_0^1$, $R_0^2 + |\overrightarrow{\mathbf{0^2 1^2}}| = R_1$, and $R_0^2 + |\overrightarrow{\mathbf{0^2 1^1}}| > R_1$. Therefore, 1^2 is obtained by rotating 1^1 counterclockwise around the center (point 2) of trace circle T_2 by an angle θ along T_2. As a result, A_5^2 is obtained by rotating A_5^1 counterclockwise around the center (point 2) of side circle 2 by an angle θ on the circumference of side circle 2. Let the straight line $1^2 0^2 A_4^2$ intersect the middle circular arc $\widehat{A_4^1A_5^1}$ at point A_4^3; let the straight line $A_5^2 1^2 2$ intersect the same circular arc at point A_5^3. It can be proven that both A_4^2 and A_5^2 lie outside the middle circle 1^1 or the middle circular arc $\widehat{A_4^1A_4^3A_5^3A_5^1}$. Therefore, the triarc $C_2\left(\widehat{AA_4^2A_5^2A_5^1C}\right)$ strictly approaches the polyline ABC more closely than $C_1\left(\widehat{AA_4^1A_4^3A_5^3A_5^1C}\right)$ although there is an overlapping segment $\widehat{A_5^1C}$. Consequently, strict approach must occur when R_0 increases from R_0^1 to R_0^2 given that both R_1 and R_2 are fixed.

Conversely, reducing R_0 from R_0^2 to R_0^1 causes the triarc C_2 to move away from the control polyline ABC, leading to an anti-strict approach. □

3.2.2.3 Proof for Type 3 by Varying One Factor R_0

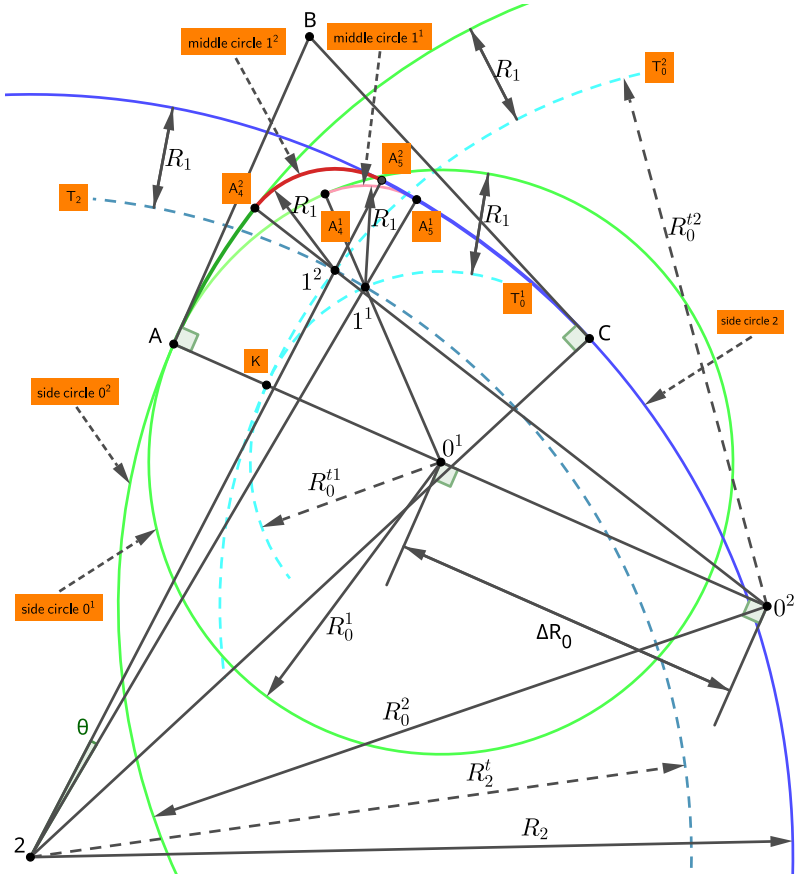

Figure 15: **Type 3 Strict Approach for R_0 ↗.** $|\overrightarrow{\mathbf{AB}}| \le |\overrightarrow{\mathbf{BC}}|$. The middle circle 1^1 is internally tangent to side circles 0^1 and 2 at points A_4^1 and A_5^1, respectively; the middle circle 1^2 is internally tangent to side circles 0^2 and 2 at points A_4^2 and A_5^2, respectively. The triarc $C_2\left(\widehat{AA_4^2A_5^2A_5^1C}\right) = \widehat{AA_4^2}$ (side circular arc) + $\widehat{A_4^2A_5^2}$ (middle circular arc) + $\widehat{A_5^2A_5^1C}$ (side circular arc); the triarc $C_1\left(\widehat{AA_4^1A_5^1C}\right) = \widehat{AA_4^1}$ (side circular arc) + $\widehat{A_4^1A_5^1}$ (middle circular arc) + $\widehat{A_5^1C}$ (side circular arc). C_2 strictly approaches the polyline ABC more closely than C_1 when R_0 increases from R_0^1 to R_0^2 given that both R_1 and R_2 are fixed. Notation follows Notation1.

Proof for ***Type 3*** *Triarcs (Fig. 15).* Suppose that the middle circle 1^1 with the radius R_1 is tangent to side circles 0^1 and 2 at points A_4^1 and A_5^1, respectively; the middle circle 1^2 with the radius R_1 is tangent to side circles 0^2 and 2 at points A_4^2 and A_5^2, respectively. When R_0 increases from R_0^1 to R_0^2 by $\triangle R_0$, the center (point 1^1) of the middle circle 1^1 must rotate along the trace circle T_2 counterclockwise around the center (point 2) of trace circle T_2 by an angle θ to 1^2 that is on T_0^2 because, firstly, $R_0^{t2} > R_0^{t1}$; and secondly, T_0^2 and T_0^1

share the tangent point K on the straight-line segment $A0^10^2$. Let the straight line 1^22 intersect side circle 2 at point A_5^2. A_5^2 is outside the triarc $C_1\left(\widehat{AA_4^1A_5^1C}\right)$ as A_5^2 is actually obtained by rotating A_5^1 counterclockwise around the center (point 2) of side circle 2 by an angle θ on the circumference of side circle 2. Let the straight line 0^21^2 intersect side circle 0^2 at point A_4^2. A_4^2 is outside the triarc C_1 because, firstly, $R_0^2 > R_0^1$; and secondly, both side circles 0^1 and 0^2 share the tangent point A. As a result, the circular arc $\widehat{A_4^2A_5^2}$ is outside the triarc C_1 because, firstly, both points A_4^2 and A_5^2 are outside the triarc C_1; and secondly, the curvature of $\widehat{A_4^2A_5^2}$ is equal to that of $\widehat{A_4^1A_5^1}$ but greater than that of $\widehat{AA_4^1}$ due to $R_1 < R_0^1$. Therefore, the triarc $C_2\left(\widehat{AA_4^2A_5^2A_5^1C}\right)$ strictly approaches the polyline ABC more closely than $C_1\left(\widehat{AA_4^1A_5^1C}\right)$ although there is an overlapping segment: $\widehat{A_5^1C}$. Consequently, strict approach must occur when R_0 increases from R_0^1 to R_0^2 given that both R_1 and R_2 are fixed.

Conversely, reducing R_0 from R_0^2 to R_0^1 causes the triarc C_2 to move away from the control polyline ABC, leading to an anti-strict approach. □

3.2.3 Strict Approach Theorem for Varying One Factor R_2

Theorem 3.3 (One-Factor Strict Approach Theorem by Varying R_2)**.** For a C-shaped triarc of **Type 1** (Fig. 16), **Type 2** (Fig. 17), or **Type 3** (Fig. 18) constructed within $\triangle ABC$, subject to the appropriate edge-length conditions:

- $|\overrightarrow{\mathbf{AB}}| \le |\overrightarrow{\mathbf{BC}}|$ (for **Type 1** and **Type 3**).
- $|\overrightarrow{\mathbf{AB}}| < |\overrightarrow{\mathbf{BC}}|$ (for **Type 2**).

given that the middle circular arc radius R_1 and the side circular arc radius R_0 are fixed:

1. When the side circular arc radius R_2 increases, the triarc must strictly approach its control polyline ABC.
2. When the side circular arc radius R_2 decreases, the triarc must strictly anti-approach its control polyline ABC.

This theorem can be proven separately for the three types of C-shaped triarcs.

3.2.3.1 Proof for Type 1 by Varying One Factor R_2

The proof of Theorem 3.3 for **Type 1** (Fig. 16) is omitted for brevity. It is analogous to the proof of Theorem 3.2 of **Type 1** (Proof 3.2.2.1) by a symmetrical argument, interchanging the roles of R_0 (and circle 0) and R_2 (and circle 2).

3.2.3.2 Proof for Type 2 by Varying One Factor R_2

*Proof for **Type 2** Triarcs (Fig. 17).* Suppose that the middle circle 1^1 with the radius R_1 is tangent to side circles 0 and 2^1 at points A_4^1 and A_5^1, respectively; the middle circle 1^2 with the radius R_1 is tangent to side circles 0 and 2^2 at points A_4^2 and A_5^2, respectively. When R_2 increases from R_2^1 to R_2^2 by $\triangle R_2$, the center (point 1^1) of the middle circle 1^1 should rotate counterclockwise around the center (point 0) of trace circle T_0 by an angle θ along T_0 to 1^2 that is on T_2^2 because, firstly, $R_2^{t2} > R_2^{t1}$; and secondly, T_2^2 and T_2^1 are tangent at point K. Therefore, point A_4^2 is obtained by rotating A_4^1 counterclockwise around the center (point 0) of side circle 0 by the same angle θ on the circumference of side circle 0. Let the straight line 2^21^2 intersect side circle 2^2 at point A_5^2. Obviously, A_5^2 is outside side circle 2^1 because, firstly, $R_2^2 > R_2^1$; and secondly, both side circles 2^1 and 2^2 are tangent at point C. Let the straight line $1^10A_4^1$ intersect the middle circle 1^2 or the middle

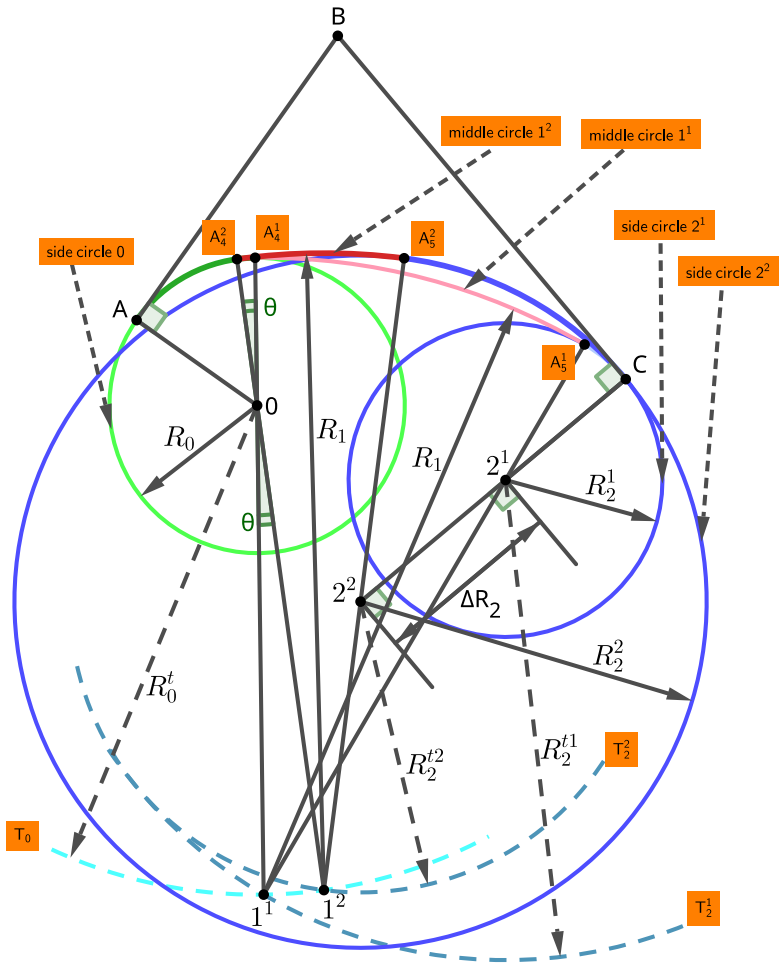

Figure 16: **Type 1 Strict Approach for R_2 ↗.** $|\overrightarrow{AB}| \leq |\overrightarrow{BC}|$. Side circles 0 and 2^1 are internally tangent to the middle circle 1^1 at points A_4^1 and A_5^1, respectively; side circles 0 and 2^2 are internally tangent to the middle circle 1^2 at points A_4^2 and A_5^2, respectively. The triarc $C_2\left(\widehat{AA_4^2A_5^2C}\right) = \widehat{AA_4^2}$ (side circular arc) + $\widehat{A_4^2A_5^2}$ (middle circular arc) + $\widehat{A_5^2C}$ (side circular arc); the triarc $C_1\left(\widehat{AA_4^2A_4^1A_5^1C}\right) = \widehat{AA_4^2A_4^1}$ (side circular arc) + $\widehat{A_4^1A_5^1}$ (middle circular arc) + $\widehat{A_5^1C}$ (side circular arc). C_2 strictly approaches the polyline ABC more closely than C_1 when R_2 increases from R_2^1 to R_2^2 given that both R_0 and R_1 are fixed. Notation follows Notation1.

circular arc $\widehat{A_4^2A_5^2}$ at point A_4^3. A_4^3 is outside side circle 0 or the circular arc $\widehat{A_4^2A_4^1}$ because, firstly, the curvature of the circular arc $\widehat{A_4^2A_4^1}$ is larger than that of the circular arc $\widehat{A_4^2A_4^3}$ as $R_0 < R_1$; and secondly, both the circular arcs $\widehat{A_4^2A_4^1}$ and $\widehat{A_4^2A_4^3}$ are tangent at point A_4^2. Let the straight line $2^11^1A_5^1$ intersect the middle circle 1^2 or the middle circular arc $\widehat{A_4^2A_4^3A_5^2}$ at point A_5^3. It is proven that A_5^3 is outside the triarc $C_1\left(\widehat{AA_4^2A_4^1A_5^1C}\right)$. Therefore, the triarc $C_2\left(\widehat{AA_4^2A_4^3A_5^3A_5^2C}\right)$ strictly approaches the polyline ABC more closely than $C_1\left(\widehat{AA_4^2A_4^1A_5^1C}\right)$ although

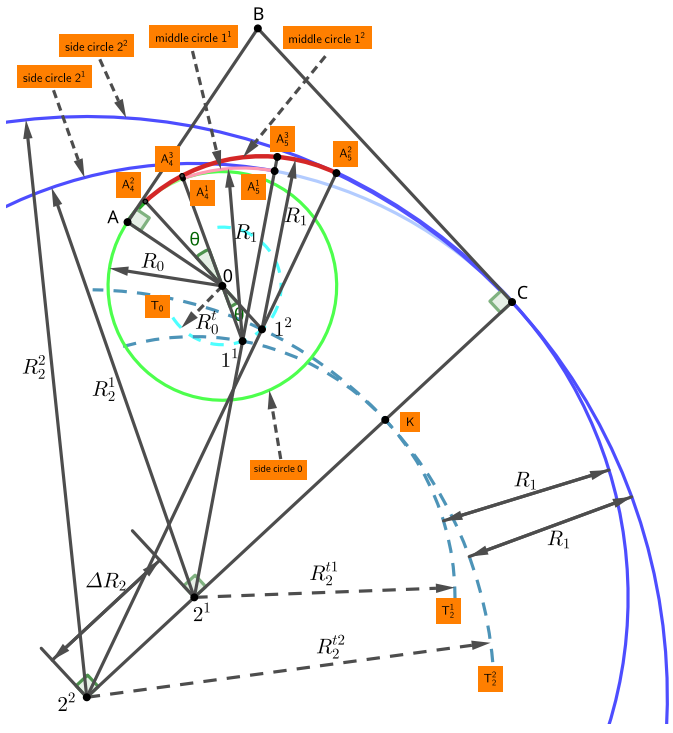

Figure 17: **Type 2 Strict Approach for R_2 ↗.** $|\overrightarrow{\mathbf{AB}}| < |\overrightarrow{\mathbf{BC}}|$. Side circle 0 is internally tangent to both middle circles 1^1 (internally tangent to side circle 2^1) and 1^2 (internally tangent to side circle 2^2). The middle circle 1^1 is tangent to side circles 0 and 2^1 at points A_4^1 and A_5^1, respectively; the middle circle 1^2 is tangent to side circles 0 and 2^2 at points A_4^2 and A_5^2, respectively. The triarc $C_2\left(\overset{\frown}{AA_4^2A_4^3A_5^3A_5^2C}\right) = \overset{\frown}{AA_4^2}$ (side circular arc) $+ \overset{\frown}{A_4^2A_4^3A_5^3A_5^2}$ (middle circular arc) $+ \overset{\frown}{A_5^2C}$ (side circular arc); the triarc $C_1\left(\overset{\frown}{AA_4^2A_4^1A_5^1C}\right) = \overset{\frown}{AA_4^2A_4^1}$ (side circular arc) $+ \overset{\frown}{A_4^1A_5^1}$ (middle circular arc) $+ \overset{\frown}{A_5^1C}$ (side circular arc). C_2 strictly approaches the polyline ABC more closely than C_1 when R_2 increases from R_2^1 to R_2^2 given that both R_0 and R_1 are fixed. Notation follows Notation1.

there is an overlapping segment: $\overset{\frown}{AA_4^2}$. Consequently, strict approach must occur when R_2 increases from R_2^1 to R_2^2 given that both R_0 and R_1 are fixed.

Conversely, reducing R_2 from R_2^2 to R_2^1 causes the triarc C_2 to move away from the control polyline ABC, leading to an anti-strict approach. □

3.2.3.3 Proof for Type 3 by Varying One Factor R_2

The proof of Theorem 3.3 for **Type 3** (Fig. 18) is omitted for brevity. It is analogous to the proof of Theorem 3.2 of **Type 3** (Proof 3.2.2.3) by a symmetrical argument, interchanging the roles of R_0 (and circle 0) and R_2 (and circle 2).

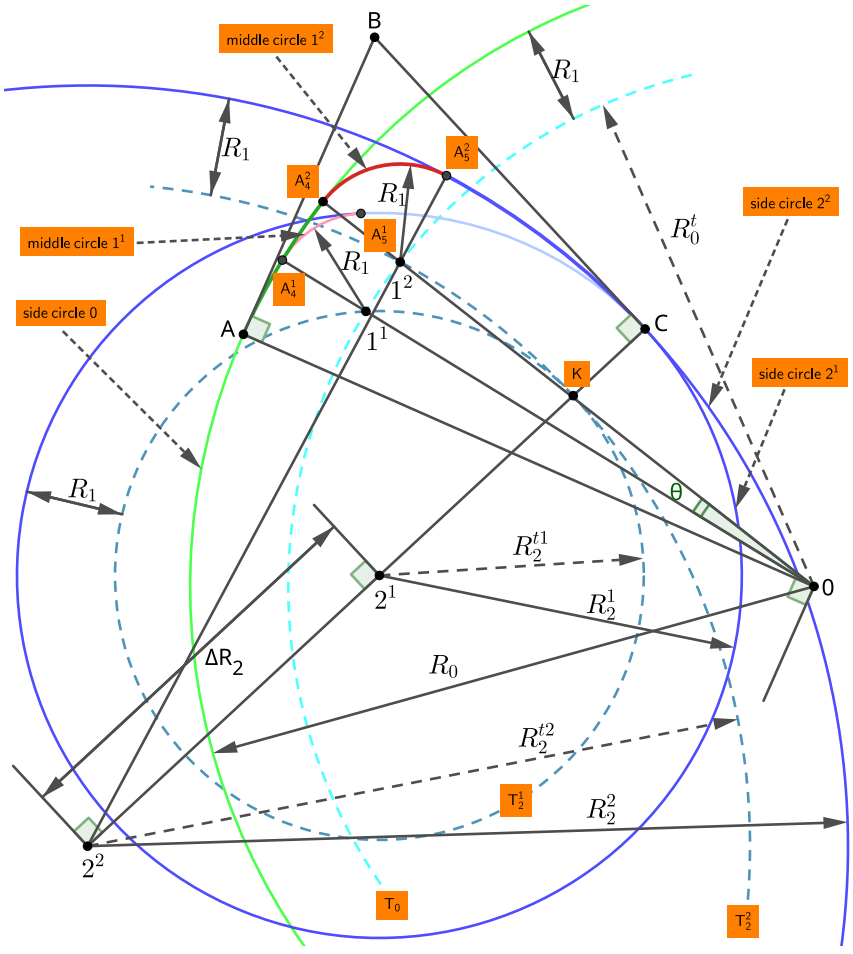

Figure 18: **Type 3 Strict Approach for R_2 ↗.** $|\overrightarrow{\mathbf{AB}}| \leq |\overrightarrow{\mathbf{BC}}|$. The middle circle 1^1 is internally tangent to side circles 0 and 2^1 at points A_4^1 and A_5^1, respectively; the middle circle 1^2 is internally tangent to side circles 0 and 2^2 at points A_4^2 and A_5^2, respectively. The triarc $C_2\left(\widehat{AA_4^1A_4^2A_5^2C}\right)$ = $\widehat{AA_4^1A_4^2}$ (side circular arc) + $\widehat{A_4^2A_5^2}$ (middle circular arc) + $\widehat{A_5^2C}$ (side circular arc); the triarc $C_1\left(\widehat{AA_4^1A_5^1C}\right)$ = $\widehat{AA_4^1}$ (side circular arc) + $\widehat{A_4^1A_5^1}$ (middle circular arc) + $\widehat{A_5^1C}$ (side circular arc). C_2 strictly approaches the polyline ABC more closely than C_1 when R_2 increases from R_2^1 to R_2^2 given that both R_0 and R_1 are fixed. Notation follows Notation1.

3.2.4 Summary of One-Factor Strict Approach Theorems by Varying $\mathbf{R_0}$, $\mathbf{R_1}$, or $\mathbf{R_2}$

Within $\triangle ABC$, **Type 1**, **Type 2**, and **Type 3** C-shaped triarcs can be generated after three factors, R_0, R_1, and R_2, are determined by the equations in Sections 2.2 and 2.3. The triarcs can strictly approach the polyline ABC if any one of R_0, R_1, or R_2 is changed in the following ways: R_0 increases, R_1 decreases, or R_2 increases, while the other two factors remain fixed according to the strict approach Theorems 3.2, 3.1, and 3.3.

Instead, in reverse of the strict approach property, triarcs also possess the anti-strict approach property, meaning that triarcs can strictly move farther away from the polyline ABC if any one of R_0, R_1, or R_2 is

changed in the reverse ways: R_0 decreases, R_1 increases, or R_2 decreases, while the other two factors remain fixed.

Table 2 summarizes how to accomplish strict approach and anti-strict approach by showing the resulting radius change when adjusting the values of the approach coefficients: α_0, α_1, and α_2.

Table 2: Effects of modifying approach coefficients on radii and approach modes (strict and anti-strict Cases).

Coefficient Modification	Fixed Radii (R_i)	Effect on Radii	Approach Mode
$\alpha_0 \nearrow$	R_1, R_2	$R_0 \nearrow$	Strict
$\alpha_1 \nearrow$	R_0, R_2	$R_1 \searrow$	
$\alpha_2 \nearrow$	R_0, R_1	$R_2 \nearrow$	
$\alpha_0 \searrow$	R_1, R_2	$R_0 \searrow$	Anti-strict
$\alpha_1 \searrow$	R_0, R_2	$R_1 \nearrow$	
$\alpha_2 \searrow$	R_0, R_1	$R_2 \searrow$	

Note: $\nearrow$ denotes an increase, and $\searrow$ denotes a decrease.

Triarcs can strictly approach or anti-approach the polyline ABC seamlessly by changing only one of R_0, R_1, or R_2. However, the changing range of the triarcs is limited as only one of three factors, R_0, R_1, or R_2, is changed. To increase the changing range of the triarcs within a triangle, more factors should be changed simultaneously for constructing more flexible triarcs. More approach theorems are proposed for this purpose.

3.3 Two-Factor Strict Approach Theorem by Varying R_0 and R_1, or R_1 and R_2

Theorem 3.4 (Two-Factor Strict Approach)**.** For a C-shaped triarc of **Type 1**, **Type 2**, or **Type 3** constructed within $\triangle ABC$, subject to the appropriate edge-length conditions:

- $|\overrightarrow{\mathbf{AB}}| \leq |\overrightarrow{\mathbf{BC}}|$ (for **Type 1** and **Type 3**).
- $|\overrightarrow{\mathbf{AB}}| < |\overrightarrow{\mathbf{BC}}|$ (for **Type 2**).

modifying two factors among R_0, R_1, and R_2 in the following ways–$R_0 \nearrow$ and $R_1 \searrow$, or $R_1 \searrow$ and $R_2 \nearrow$ while keeping the third factor fixed–can result in the triarc strictly approaching its control polyline ABC in a more precise and adjustable strict approach manner. Conversely, reversing the modifications ($R_0 \searrow$ and $R_1 \nearrow$,or $R_1 \nearrow$ and $R_2 \searrow$) leads to an anti-strict approach.

Proof. The two-factor strict approach property is a cumulative effect derived from the established one-factor strict approach theorems (Section 3.2).

- Case 1: $R_0 \nearrow$ and $R_1 \searrow$. Modifying $R_0 \nearrow$ (Theorem 3.2) and $R_1 \searrow$ (Theorem 3.1) simultaneously results in two strict approaches. Since both actions move the triarc closer to the polyline ABC, their combined effect is a guaranteed strict approach.
- Case 2: $R_1 \searrow$ and $R_2 \nearrow$. Similarly, the combined strict approach effects of $R_1 \searrow$ (Theorem 3.1) and $R_2 \nearrow$ (Theorem 3.3) also guarantee an overall strict approach.

The anti-strict approach property is proven by the same logic, as the reversed modifications ($R_0 \searrow$ and $R_1 \nearrow$, or $R_1 \nearrow$ and $R_2 \searrow$) result in the accumulation of two anti-strict approaches, moving the triarc farther away from the polyline ABC. □

3.4 Two-Factor Advanced Approach Theorem by Varying $\mathbf{R_0}$ and $\mathbf{R_2}$

Theorem 3.5 (Two-Factor Advanced Approach)**.** For a C-shaped triarc of **Type 1**, **Type 2**, or **Type 3** constructed within $\triangle ABC$, subject to the appropriate edge-length conditions:

- $|\overrightarrow{\mathbf{AB}}| \leq |\overrightarrow{\mathbf{BC}}|$ (for **Type 1** and **Type 3**).
- $|\overrightarrow{\mathbf{AB}}| < |\overrightarrow{\mathbf{BC}}|$ (for **Type 2**).

modifying two factors R_0 and R_2 in the following way–$R_0 \nearrow$ and $R_2 \nearrow$ while keeping the third factor R_1 fixed–can result in the triarc completely approaching its control polyline ABC in an advanced approach manner. Conversely, reversing the modification ($R_0 \searrow$ and $R_2 \searrow$) leads to an anti-advanced approach.

Proof. The two-factor advanced approach property is a cumulative and synergistic effect derived from the established one-factor strict approach theorems (Section 3.2). This is demonstrated by examining the simultaneous increase of R_0 and R_2 while R_1 remains fixed.

- Effect of $R_0 \nearrow$: $R_0 \nearrow$ strictly moves the arc associated with R_0 closer to edge AB (Theorem 3.2).
- Effect of $R_2 \nearrow$: $R_2 \nearrow$ strictly moves the arc associated with R_2 closer to edge BC (Theorem 3.3).

Since both simultaneous changes force the two side circular arcs to shift inward toward their respective edges, the G^1 continuity constraint of the triarc implies that the middle circular arc (with fixed R_1) must also shift inward, moving closer to the vertex B and the control polyline ABC. This accumulated inward movement guarantees a complete advanced approach.

The anti-advanced approach property is proven by the same logic: reversing the modifications ($R_0 \searrow$ and $R_2 \searrow$) results in the accumulation of two anti-strict approaches, which forces the triarc farther away from the polyline ABC. □

3.5 Three-Factor Advanced Approach Theorem by Varying $\mathbf{R_0}$, $\mathbf{R_1}$, and $\mathbf{R_2}$

Building upon the enhanced adjustability demonstrated by varying two factors, the most comprehensive and effective method is to modify all three factors simultaneously. This work therefore proposes the simultaneous adjustment of the three approach coefficients, α_0 for R_0, α_1 for R_1, and α_2 for R_2, to achieve maximal control.

Theorem 3.6 (Three-Factor Advanced Approach)**.** For a C-shaped triarc of **Type 1**, **Type 2**, or **Type 3** constructed within $\triangle ABC$, subject to the appropriate edge-length conditions:

- $|\overrightarrow{\mathbf{AB}}| \leq |\overrightarrow{\mathbf{BC}}|$ (for **Type 1** and **Type 3**).
- $|\overrightarrow{\mathbf{AB}}| < |\overrightarrow{\mathbf{BC}}|$ (for **Type 2**).

simultaneously modifying all three factors R_0, R_1, and R_2 in the following way–$R_0 \nearrow$, $R_1 \searrow$, and $R_2 \nearrow$–causes the triarc to completely approach its control polyline ABC in an advanced approach manner. Conversely, reversing the modification ($R_0 \searrow$, $R_1 \nearrow$, and $R_2 \searrow$) leads to an anti-advanced approach.

Proof. The three-factor advanced approach property is a maximally cumulative effect derived from the established one-factor strict approach theorems (Section 3.2). This is demonstrated by examining the simultaneous modification of all three radii in the stated directions:

- Effect of R_0 ↗: R_0 ↗ strictly moves the arc associated with R_0 closer to edge AB (Theorem 3.2).
- Effect of R_1 ↘: R_1 ↘ strictly moves the arc associated with R_1 closer to the vertex B and to the polyline ABC (Theorem 3.1).
- Effect of R_2 ↗: R_2 ↗ strictly moves the arc associated with R_2 closer to edge BC (Theorem 3.3).

Since all three simultaneous changes act in the same direction–driving each respective circular arc closer to the control polyline ABC–their accumulated effect guarantees the most comprehensive advanced approach of the entire triarc to the polyline ABC.

The anti-advanced approach property is proven by the same logic, as the reversed modifications (R_0 ↘, R_1 ↗, and R_2 ↘) result in the accumulation of three anti-strict approaches, which forces the triarc farther away from the polyline ABC. □

4 DEMONSTRATIVE RESULTS

This section demonstrates the various approach methods–general, strict (one- or two-factor), and advanced (two- or three-factor)–for **Type 1**, **Type 2**, and **Type 3** C-shaped triarcs. It concludes with examples of degenerated biarcs and final triarc curves. All strict and advanced approach examples also serve to illustrate the corresponding anti-strict and anti-advanced approaches when the modifications (changes to approach coefficients $\alpha_0, \alpha_1, \alpha_2$) are reversed.

The approach coefficients function as independent shape control parameters, where increasing each parameter drives the triarc closer to a specific feature:

- α_0: edge AB.
- α_1: vertex B.
- α_2: edge BC.

Conversely, decreasing these parameters pulls the triarcs farther away from their respective features.

All subsequent **Type 3** examples are based on the R_0 and R_2 construction method detailed in Section 2.2.3.2.

4.1 Examples of General Approach

Random adjustments of the shape control parameters α_0, α_1, and α_2 may lead to general or anti-general approach modes of C-shaped triarcs. Fig. 19 illustrates a few examples.

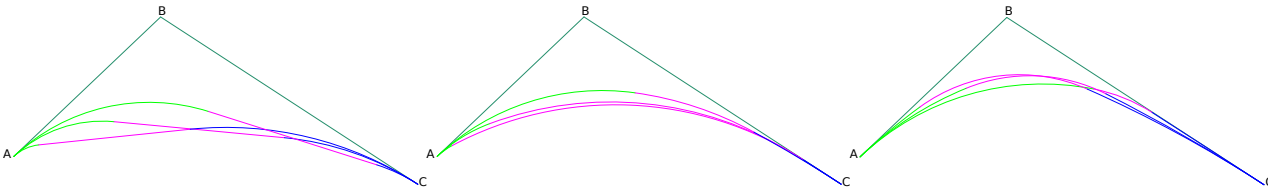

(a) **Type 1:** Base triarc: (α_0, α_1, α_2) = (0.5, 0.5, 2.5). R_0 ↗ and R_2 ↘ with (α_0, α_2) = (1.5, 2), (2.5, 1.5).

(b) **Type 2:** Base triarc: (α_0, α_1, α_2) = (3.8, 4.5, 5.8). R_0 ↗ and R_2 ↘ with (α_0, α_2) = (4.8, 4.8), (5.8, 3.5).

(c) **Type 3:** Base triarc: (α_0, α_1, α_2) = (6.1, 12.0, 150.0). R_0 ↗ and R_2 ↘ with (α_0, α_2) = (7, 15.0), (10, 2.0).

Figure 19: General approach examples of radii counter-directional modifications: R_0 ↗ and R_2 ↘ with fixed R_1. The resulting triarcs approach AB while receding from BC. The approach to polyline ABC is non-strict and non-advanced, resulting in triarc intersections.

4.2 Examples of One-Factor Strict Approach by Varying R_0, R_1, or R_2

One-Factor Strict approach is achieved by changing only one radius factor (R_0, R_1, or R_2) while the others remain fixed, as proven by Theorems 3.2, 3.1, and 3.3. Figure 20 illustrates this principle across all three triarc types, showing how adjusting the corresponding approach coefficient in the required direction ($\alpha_0 \nearrow \Longrightarrow R_0 \nearrow$, $\alpha_1 \nearrow \Longrightarrow R_1 \searrow$, or $\alpha_2 \nearrow \Longrightarrow R_2 \nearrow$) causes the triarcs to strictly and monotonically approach the polyline ABC.

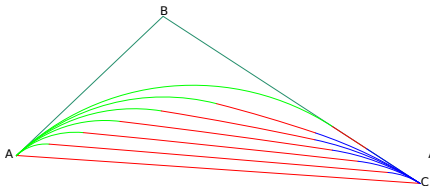

(a) **Type 1** (Theorem 3.2): Base triarc: $\alpha_0 = \alpha_1 = \alpha_2 = 0.01$. $R_0 \nearrow$ with $\alpha_0 = 0.5, 1, 1.5, 2, 2.5, 2.99$.

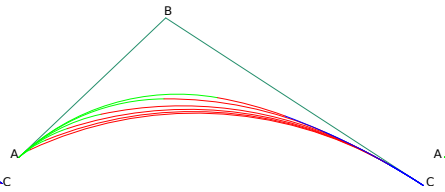

(b) **Type 2** (Theorem 3.2): Base triarc: $\alpha_0 = \alpha_1 = \alpha_2 = 3.5$. $R_0 \nearrow$ with $\alpha_0 = 4, 4.5, 5, 5.5, 5.7$.

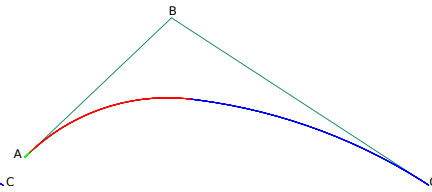

(c) **Type 3** (Theorem 3.2): Base triarc: $\alpha_0 = \alpha_1 = \alpha_2 = 7$. $R_0 \nearrow$ with $\alpha_0 = 9, 11, 15, 25, 46, 70, 100$.

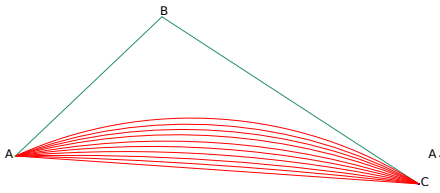

(d) **Type 1** (Theorem 3.1): Base triarc: $\alpha_0 = \alpha_1 = \alpha_2 = 0.01$. $R_1 \searrow$ with $\alpha_1 = 2, 2.3, 2.5, 2.64, 2.74, 2.83, 2.89, 2.94, 2.99$.

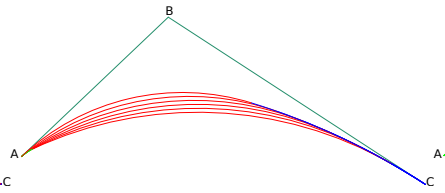

(e) **Type 2** (Theorem 3.1): Base triarc: $\alpha_0 = \alpha_1 = \alpha_2 = 3.5$. $R_1 \searrow$ with $\alpha_1 = 4, 4.5, 5, 5.5, 5.99$.

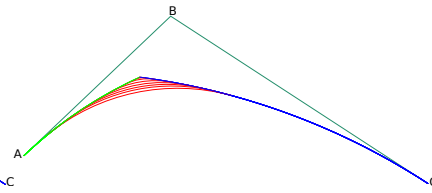

(f) **Type 3** (Theorem 3.1): Base triarc: $\alpha_0 = \alpha_1 = \alpha_2 = 8$. $R_1 \searrow$ with $\alpha_1 = 10, 12, 15, 20, 30, 45, 70, 200$.

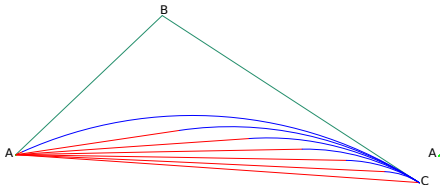

(g) **Type 1** (Theorem 3.3): Base triarc: $\alpha_0 = \alpha_1 = \alpha_2 = 0.01$. $R_2 \nearrow$ with $\alpha_2 = 0.5, 1, 1.5, 2, 2.5, 2.99$.

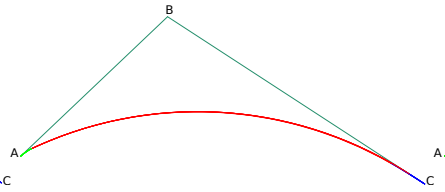

(h) **Type 2** (Theorem 3.3): Base triarc: $\alpha_0 = \alpha_1 = \alpha_2 = 3.5$. $R_2 \nearrow$ with $\alpha_2 = 4, 4.5, 5, 5.5, 5.99$.

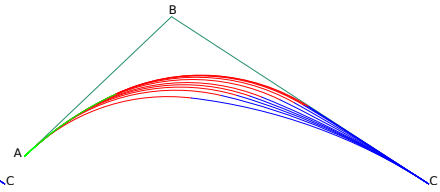

(i) **Type 3** (Theorem 3.3): Base triarc: $\alpha_0 = \alpha_1 = \alpha_2 = 7$. $R_2 \nearrow$ with $\alpha_2 = 7.7, 8.3, 9, 10, 13, 20, 40, 70, 120$.

Figure 20: One-factor strict approach examples of changing one factor: $R_0 \nearrow$, $R_1 \searrow$, or $R_2 \nearrow$. The resulting triarcs strictly and monotonically approach the polyline ABC: each successive triarc lies strictly between its predecessor and the polyline ABC. Overlapping only happens on the fixed arc segments.

4.3 Examples of Two-Factor Strict Approach by Varying R_0 and R_1, or R_1 and R_2

Two-factor strict approach can be implemented by simultaneously changing only two radii factors: R_0 and R_1, or R_1 and R_2, as detailed in Theorem 3.4. The resulting triarcs strictly and monotonically approach the polyline ABC. Figure 21 illustrates these examples, showing how altering the corresponding approach coefficients (α_0, α_1, or α_2) in the required direction achieves this strict approach.

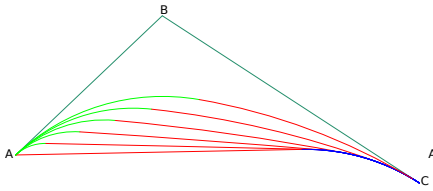

(a) **Type 1** (Theorem 3.4): Base triarc: $\alpha_0 = \alpha_1 = \alpha_2 = 0.01$ and then α_2 =1.5. $R_0 \nearrow$ and $R_1 \searrow$ with $(\alpha_0,\ \alpha_1) = (0.5,\ 0.8),\ (1.0,\ 1.6),\ (1.5,\ 2.3),\ (2.0,\ 2.7),\ (2.5,\ 2.95)$.

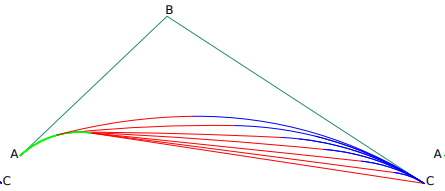

(b) **Type 1** (Theorem 3.4): Base triarc: $\alpha_0 = \alpha_1 = \alpha_2 = 0.01$ and then $\alpha_0 = 1.0$. $R_1 \searrow$ and $R_2 \nearrow$ with $(\alpha_1,\ \alpha_2) = (0.5,\ 0.5),\ (1.0,\ 1.0),\ (1.5,\ 1.5),\ (2.0,\ 2.0),\ (2.5,\ 2.5),\ (2.9,\ 2.9)$.

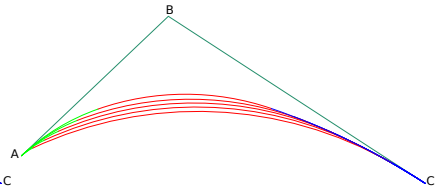

(c) **Type 2** (Theorem 3.4): Base triarc: $\alpha_0 = \alpha_1 = \alpha_2 = 3.5$. $R_0 \nearrow$ and $R_1 \searrow$ with $(\alpha_0,\ \alpha_1) = (4.0,\ 4.0),\ (4.5,\ 4.5),\ (5.0,\ 5.0),\ (5.5,\ 5.7)$.

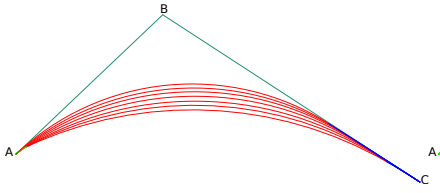

(d) **Type 2** (Theorem 3.4): Base triarc: $\alpha_0 = \alpha_1 = \alpha_2 = 3.5$. $R_1 \searrow$ and $R_2 \nearrow$ with $(\alpha_1,\ \alpha_2) = (4.0,\ 4.0),\ (4.5,\ 4.5),\ (5.0,\ 5.0),\ (5.4,\ 5.4),\ (5.7,\ 5.7),\ (5.99,\ 5.99)$.

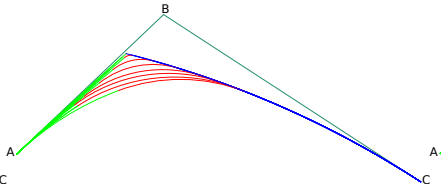

(e) **Type 3** (Theorem 3.4): Base triarc: $\alpha_0 = \alpha_1 = \alpha_2 = 6.5$ and then $\alpha_2 = 10$. $R_0 \nearrow$ and $R_1 \searrow$ with $(\alpha_0,\ \alpha_1) = (8,\ 11),\ (11,\ 13),\ (13,\ 16),\ (16,\ 22),\ (22,\ 32),\ (32,\ 55),\ (55,\ 130)$.

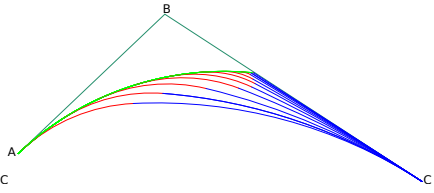

(f) **Type 3** (Theorem 3.4): Base triarc: $\alpha_0 = \alpha_1 = \alpha_2 = 6.5$. $R_1 \searrow$ and $R_2 \nearrow$ with $(\alpha_1,\ \alpha_2) = (8,\ 7),\ (10,\ 8),\ (12,\ 10),\ (15,\ 13),\ (20,\ 18),\ (28,\ 25),\ (45,\ 40),\ (85,\ 70),\ (125,\ 200)$.

Figure 21: Two-factor strict approach examples of changing two factors: $R_0 \nearrow$ and $R_1 \searrow$, or $R_1 \searrow$ and $R_2 \nearrow$. The resulting triarcs strictly and monotonically approach the polyline ABC: each successive triarc lies strictly between its predecessor and the polyline ABC (overlapping along the single fixed arc segment).

4.4 Examples of Two-Factor Advanced Approach by Varying $\mathbf{R_0}$ and $\mathbf{R_2}$

Two-factor advanced approach is implemented by simultaneously changing only the two side radii factors, R_0 and R_2, while keeping R_1 fixed, as established in Theorem 3.5. Figure 22 illustrates these examples across the three triarc types, where altering the approach coefficients α_0 and α_2 ($\alpha_0 \nearrow \Longrightarrow R_0 \nearrow$, $\alpha_2 \nearrow \Longrightarrow R_2 \nearrow$) causes the triarcs to approach the polyline ABC advancedly and strictly monotonically.

4.5 Examples of Three-Factor Advanced Approach by Varying $\mathbf{R_0}$, $\mathbf{R_1}$, and $\mathbf{R_2}$

Three-factor advanced approach is implemented by simultaneously changing all three radii factors, R_0, R_1, and R_2, as detailed in Theorem 3.6. Figure 23 illustrates the advanced and strictly monotonic approach examples by adjusting all three approach coefficients ($\alpha_0 \nearrow \Longrightarrow R_0 \nearrow$, $\alpha_1 \nearrow \Longrightarrow R_1 \searrow$, $\alpha_2 \nearrow \Longrightarrow R_2 \nearrow$).

A significant feature is illustrated in Fig. 23c: the **Type 3** C-shaped triarcs can be driven to degenerate into the control polyline ABC as $\alpha_0, \alpha_1, \alpha_2 \to +\infty$. This limit corresponds to the radii changes $R_0 \to +\infty$, $R_1 \to 0$, and $R_2 \to +\infty$.

4.6 Examples of Biarcs Degenerated from C-Shaped Triarcs

A C-shaped triarc can degenerate to a biarc when the radius R_1 of the middle circular arc is equal to the boundary radius R_{4b} or R_{5b} as described in the proposition 2 of Section 2.3.1, the propositions 2 and 3 of

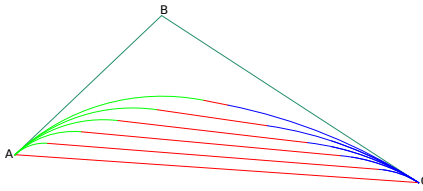

(a) **Type 1** (Theorem 3.5): Base triarc: $\alpha_0 = \alpha_1 = \alpha_2 = 0.01$. R_0 ↗ and R_2 ↗ with $(\alpha_0,\ \alpha_2)$ = (0.5, 0.6), (1.0, 1.2), (1.5, 1.75), (2.0, 2.4), (2.5, 2.95).

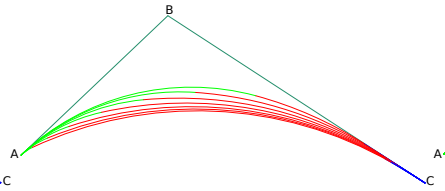

(b) **Type 2** (Theorem 3.5): Base triarc: $\alpha_0 = \alpha_1 = \alpha_2 = 3.5$. R_0 ↗ and R_2 ↗ with $(\alpha_0,\ \alpha_2)$ = (4.0, 4.0), (4.5, 4.5), (5.0, 5.0), (5.4, 5.4), (5.7, 5.7), (5.9, 5.9).

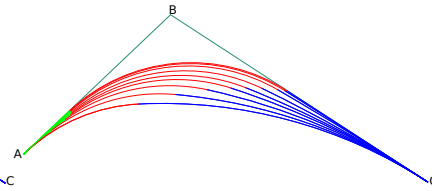

(c) **Type 3** (Theorem 3.5): Base triarc: $\alpha_0 = \alpha_1 = \alpha_2 = 6.5$. R_0 ↗ and R_2 ↗ with $(\alpha_0,\ \alpha_2)$ = (7, 7), (7.8, 7.8), (9, 9), (10.5, 10.5), (14, 14), (25, 28), (50, 80), (200, 500).

Figure 22: Two-factor advanced approach examples of changing two factors: R_0 ↗ and R_2 ↗. The resulting triarcs approach the polyline ABC advancedly and strictly monotonically: each successive triarc lies entirely between its predecessor and the polyline ABC.

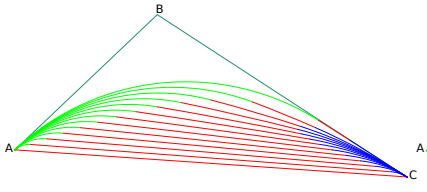

(a) **Type 1** (Theorem 3.6): Base triarc: $\alpha_0 = \alpha_1 = \alpha_2 = 0.01$. R_0 ↗, R_1 ↘, and R_2 ↗ with $\alpha_0 = \alpha_1 = \alpha_2$ = 0.25, 0.5, 0.75, 1, 1.25, 1.5, 1.75, 2, 2.25, 2.5, 2.75, 2.99.

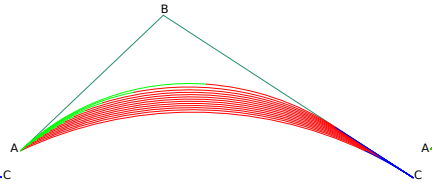

(b) **Type 2** (Theorem 3.6): Base triarc: $\alpha_0 = \alpha_1 = \alpha_2 = 3.01$. R_0 ↗, R_1 ↘, and R_2 ↗ with $\alpha_0 = \alpha_1 = \alpha_2$ = 3.25, 3.5, 3.75, 4, 4.25, 4.5, 4.75, 5, 5.25, 5.5, 5.75, 5.95.

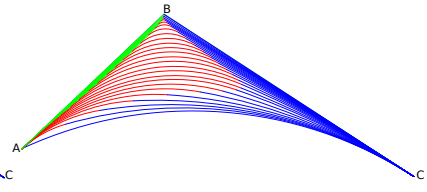

(c) **Type 3** (Theorem 3.6): Base triarc: $\alpha_0 = \alpha_1 = \alpha_2 = 6.01$. R_0 ↗, R_1 ↘, and R_2 ↗ with $\alpha_0 = \alpha_1 = \alpha_2$ = 6.15, 6.3, 6.5, 6.8, 7.3, 8, 9, 10, 11.5, 13, 15, 17, 19.5, 22, 25, 29, 34, 41, 50, 60, 75, 100, 180, 1100.

Figure 23: Three-factor advanced approach examples of changing three factors: R_0 ↗, R_1 ↘, and R_2 ↗. The resulting triarcs approach the polyline ABC advancedly and strictly monotonically: each successive triarc lies entirely between its predecessor and the polyline ABC.

Section 2.3.2, and the proposition 2 of Section 2.3.3. Fig. 24 illustrates the examples of biarcs resulting from the degeneration of C-shaped triarcs.

4.7 Example of Special Case — Single Circular Arc

Type 1, **Type 2**, and **Type 3** C-shaped triarcs can degenerate to a single circular arc within an isosceles $\triangle ABC$. Fig. 25 illustrates one degeneration case.

4.8 Examples of C-Shaped Triarc Curves

Fig. 26 illustrates the families of **Type 1**, **Type 2**, and **Type 3** triarc curves in an advanced approach manner.

Conversely, these families of triarc curves can be viewed as the anti-advanced approach instances in which the triarc curves are generated with the three approach coefficients changed in the reverse order (from larger to smaller).

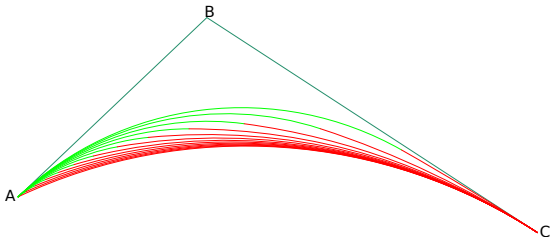

(a) **Type 1:** A family of biarcs when $R_1 = R_{5b}$ with $\alpha_0 = \alpha_1 = \alpha_2 =$ 0.01, 0.25, 0.5, 0.75, 1, 1.25, 1.5, 1.75, 2, 2.25, 2.5, 2.75, 2.95.

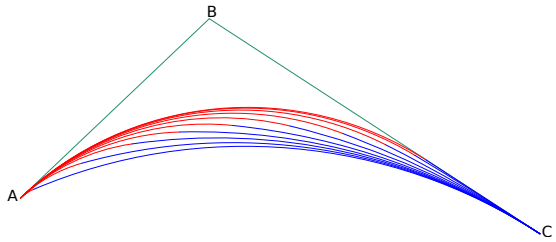

(b) **Type 2:** A family of biarcs when $R_1 = R_{4b}$ with $\alpha_0 = \alpha_1 = \alpha_2 =$ 3.01, 3.05, 3.1, 3.16, 3.25, 3.4, 3,65, 4.1, 5, 5.95.

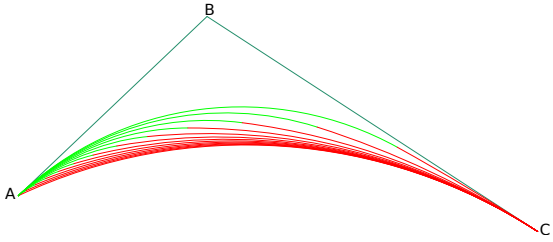

(c) **Type 2:** A family of biarcs when $R_1 = R_{5b}$ with $\alpha_0 = \alpha_1 = \alpha_2 =$ 3.01, 3.25, 3.5, 3.75, 4, 4.25, 4.5, 4.75, 5, 5.25, 5.5, 5.75, 5.95.

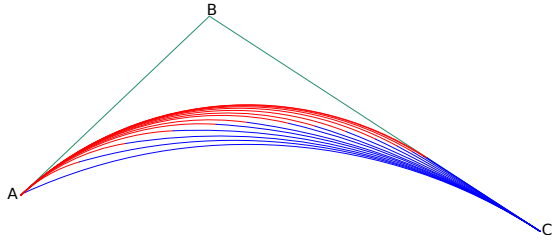

(d) **Type 3:** A family of biarcs when $R_1 = R_{4b}$ with $\alpha_0 = \alpha_1 = \alpha_2 =$ 6.01, 6.15, 6.3, 6.5, 6.75, 7, 7.5, 8, 9, 11, 15, 25, 75, 700.

Figure 24: Biarcs are the degeneration of C-shaped triarcs. The resulting biarcs advancedly and monotonically approach the polyline ABC: each successive biarc lies entirely between its predecessor and the polyline ABC.

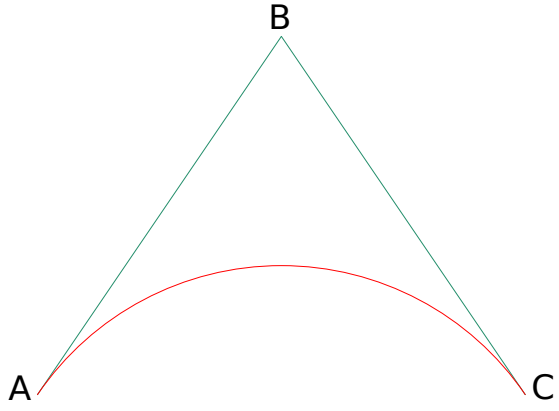

Figure 25: **Type 2:** Only one single circular arc is generated within an isosceles $\triangle ABC$ with $|\overrightarrow{\mathbf{AB}}| = |\overrightarrow{\mathbf{BC}}|$.

5 CONCLUSIONS

This paper presents a method for constructing C-shaped triarcs within a triangle. Three types of C-shaped triarcs are defined based on the tangency relationships between the middle circular arc and the two side circular arcs. Section 2 provides the detailed construction methods and establishes the necessary equations to ensure that the triarcs exhibit the desired approach properties.

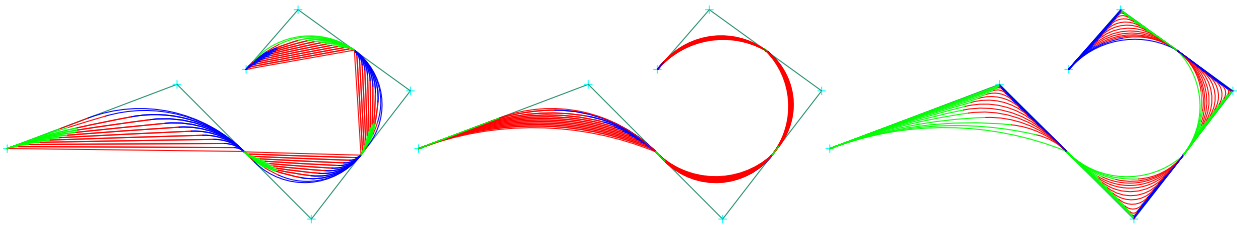

(a) **Type 1:** A family of triarc curves with $\alpha_0 = \alpha_1 = \alpha_2 = 0.018, 0.286, 0.573, 0.859, 1.145, 1.431, 1.718, 2.004, 2.290, 2.577, 2.863, 2.999$.

(b) **Type 2:** A family of triarc curves with $\alpha_0 = \alpha_1 = \alpha_2 = 3.0, 3.289, 3.579, 3.869, 4.158, 4.448, 4.738, 5.028, 5.317, 5.607, 5.897, 6.0$.

(c) **Type 3:** A family of triarc curves with $\alpha_0 = \alpha_1 = \alpha_2 = 6.01, 6.3, 6.7, 7.5, 9, 11, 14, 18, 23, 30, 41, 58, 80, 120, 300$.

Figure 26: C-shaped triarc curves completely approach their control polylines in an advanced approach manner.

For a given triangle ABC, the coefficients α_0, α_1, and α_2 define families of triarcs with additional design degrees of freedom within the G^1 interpolation constraints. Different combinations of these coefficients produce varied curves within the admissible geometric range, allowing designers to precisely adjust the proximity of the triarc to the control polyline. Table 3 lists representative parameter adjustments corresponding to the various approach modes, while the examples in Section 4 demonstrate typical parameter choices and the resulting triarc geometries.

A comprehensive set of approach concepts–general, anti-general, strict, anti-strict, advanced, and anti-advanced–within a triangle is defined in Section 3.1, and an area-based formula (Eq. 20) is introduced for evaluating the approach ratio. The strict and advanced approach theorems (Sections 3.2, 3.3, 3.4, and 3.5) guarantee monotonic, non-crossing movement of triarcs toward the two-edged control polyline, whereas the anti-strict and anti-advanced approaches represent the inverse movement.

The approach coefficients α_0, α_1, and α_2 serve as independent shape control parameters, directly governing the proximity of the triarcs to the edges AB and BC, and to vertex B of $\triangle ABC$. Table 3 summarizes how variations in these coefficients implement all approach and anti-approach modes. Additionally, triarcs may degenerate into biarcs under specific boundary conditions (A-8) or (A-13), as illustrated in Fig. 24.

Key advantages of the proposed triarc curves include:

- Full coverage of approach and anti-approach modes (general, strict, advanced, anti-general, anti-strict, and anti-advanced) with precise control via independent shape parameters α_0, α_1, and α_2.
- Guaranteed monotonic or strictly monotonic, non-crossing movement toward the two-edged control polyline in strict and advanced approach modes, respectively.
- Curves consist solely of circular arcs with simple, explicit formulas for radii (R_0, R_1, R_2).
- Convexity-preserving construction within the two-edged control polylines.
- Non-self-intersecting and inflection-free triarcs forming nested families that do not cross in strict and advanced modes, although overlapping may occur in strict mode.

The flexibility and adaptability of these triarc curves make them suitable for geometric modeling and design applications, including curve fitting and CNC machining, where precise control over curve behavior is required.

ACKNOWLEDGEMENTS

This research received no external funding.

Table 3: Effects of modifying approach coefficients on radii and the resulting approach modes for **Type 1**, **Type 2**, and **Type 3** triarcs.

Coefficient Modification	Fixed Radii	Number of Radii Modified	Directional Change in Radii	Approach Mode
α_0 ↗	R_1, R_2	1	R_0 ↗	Strict
α_1 ↗	R_0, R_2	1	R_1 ↘	
α_2 ↗	R_0, R_1	1	R_2 ↗	
α_0 ↘	R_1, R_2	1	R_0 ↘	Anti-strict
α_1 ↘	R_0, R_2	1	R_1 ↗	
α_2 ↘	R_0, R_1	1	R_2 ↘	
α_0 ↗, α_1 ↗	R_2	2	R_0 ↗, R_1 ↘	Strict
α_1 ↗, α_2 ↗	R_0	2	R_1 ↘, R_2 ↗	
α_0 ↘, α_1 ↘	R_2	2	R_0 ↘, R_1 ↗	Anti-strict
α_1 ↘, α_2 ↘	R_0	2	R_1 ↗, R_2 ↘	
α_0 ↗, α_2 ↗	R_1	2	R_0 ↗, R_2 ↗	Advanced
α_0 ↘, α_2 ↘	R_1	2	R_0 ↘, R_2 ↘	Anti-advanced
α_0 ↗, α_1 ↗, α_2 ↗	None	3	R_0 ↗, R_1 ↘, R_2 ↗	Advanced
α_0 ↘, α_1 ↘, α_2 ↘	None	3	R_0 ↘, R_1 ↗, R_2 ↘	Anti-advanced
Other combinations (see Notes)	Varies	2–3 radii	Mixed directions	General / Anti-General

Notes: ↗ denotes an increase, and ↘ denotes a decrease. **Others (General / Anti-General Modes):** Include all remaining combinations not listed above.
Two Factors Changed: (α_0↗,α_1↘), (α_0↗,α_2↘), (α_0↘,α_1↗), (α_0↘,α_2↗), (α_1↘,α_2↗), (α_1↗,α_2↘).
Three Factors Changed: (α_0↗,α_1↘,α_2↗), (α_0↗,α_1↗,α_2↘), (α_0↗,α_1↘,α_2↘), (α_0↘,α_1↗,α_2↗), (α_0↘,α_1↘,α_2↗), (α_0↘,α_1↗,α_2↘).

ORCID

Tom Guo, http://orcid.org/0009-0003-1483-0750

A APPENDIX: CALCULATIONS

For **Type 1**, **Type 2**, and **Type 3** C-shaped triarcs, the tangency relationships between middle circle 1 and two side circles 0 and 2 are depicted in Fig. A.1 in which the middle circle 1 is tangent to side circle 0 at point 4 and to side circle 2 at point 5. The triarc $\widehat{A45C}$ is composed of three minor circular arcs: $\widehat{A4}$ that is a side circular arc, $\widehat{45}$ that is a middle circular arc, and $\widehat{5C}$ that is a side circular arc.

This appendix discusses how to calculate various coordinates and the boundary radii R_{4b} and R_{5b}.

A.1 Calculate the Generic Coordinates of the Center 1 of Middle Circle 1

For the **Type 1**, **Type 2**, and **Type 3** C-shaped triarcs illustrated in Fig. A.1, the coordinates of the center (point 1) of middle circle 1 are determined by the following two equations, which define the trace circles T_0

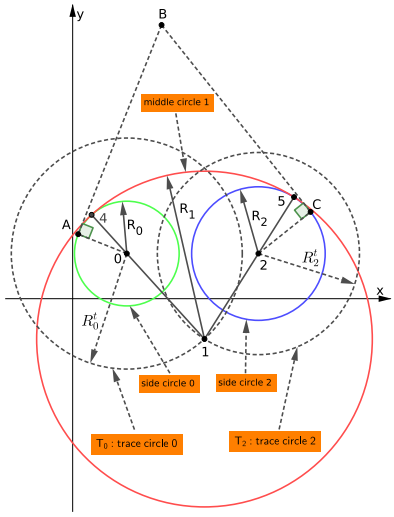

(a) **Type 1:** Both side circles 0 and 2 are internally tangent to middle circle 1. $R_0^t = R_1 - R_0$; $R_2^t = R_1 - R_2$.

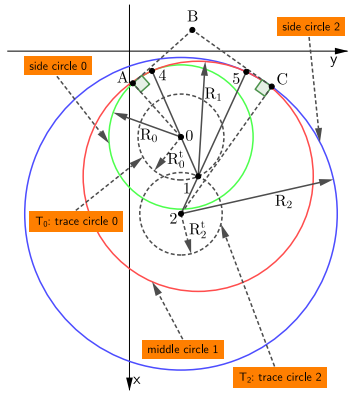

(b) **Type 2:** Side circle 0 is internally tangent to middle circle 1 that is internally tangent to side circle 2. $R_0^t = R_1 - R_0$; $R_2^t = R_2 - R_1$.

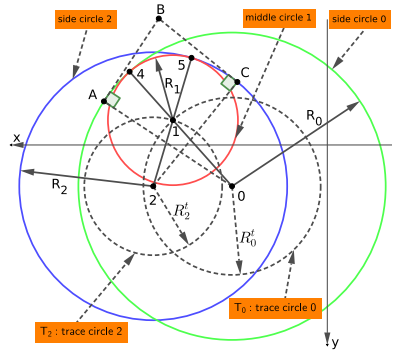

(c) **Type 3:** Middle circle 1 is internally tangent to both side circles 0 and 2. $R_0^t = R_0 - R_1$; $R_2^t = R_2 - R_1$.

Figure A.1: The tangency relationships between middle circle 1 and two side circles 0 and 2 define the three types of C-shaped triarcs within $\triangle ABC$. Side circle 0 is tangent to AB at point A and side circle 2 is tangent to BC at point C. Middle circle 1 is tangent to side circles 0 and 2 at points 4 and 5, respectively. T_0 is the trace circle of side circle 0 and T_2 is the trace circle of side circle 2. Point 1 is one of the two intersection points between the trace circles T_0 and T_2. R_0 = the radius of side circle 0; R_1 = the radius of middle circle 1; R_2 = the radius of side circle 2; R_0^t = the radius of trace circle T_0; R_2^t = the radius of trace circle T_2. The triarc $\widehat{A45C}$ is composed of three minor circular arcs: $\widehat{A4}$ (side circular arc), $\widehat{45}$ (middle circular arc), and $\widehat{5C}$ (side circular arc).

and T_2, respectively.

$$(X-X_0)^2+(Y-Y_0)^2=(\mathbf{R_0^t})^2=(R_1-R_0)^2, \quad \text{(Trace circle } T_0 \text{ with its center at 0);} \tag{A-1a}$$

$$(X-X_2)^2+(Y-Y_2)^2=(\mathbf{R_2^t})^2=(R_1-R_2)^2, \quad \text{(Trace circle } T_2 \text{ with its center at 2),} \tag{A-1b}$$

where

$(X_0,\ Y_0)$ are the coordinates of the center of side circle 0 with radius R_0,
$(X_2,\ Y_2)$ are the coordinates of the center of side circle 2 with radius R_2,
and R_1 is the radius of middle circle 1.

From Eqs. (A-1a) and (A-1b), have the coordinates (X_1, Y_1) of the center of middle circle 1:

$$Y_1=\frac{T5\cdot R_1+T6+S\sqrt{T10\cdot R_1^2+T11\cdot R_1+T12}}{1+T2^2}; \tag{A-2a}$$

$$X_1=T3\cdot R_1+T4-Y_1\cdot T2, \tag{A-2b}$$

where

$$T1=R_1\cdot T3+T4,$$

$$T2=\frac{Y_2-Y_0}{X_2-X_0}, \quad T3=\frac{R_2-R_0}{X_2-X_0},$$

$$T4=\frac{X_2^2+Y_2^2-R_2^2+R_0^2-X_0^2-Y_0^2}{2\,(X_2-X_0)},$$

$$T5=T2\cdot T3, \quad T6=-T2\cdot(X_0-T4)+Y_0,$$

$$T7=T3^2-1, \quad T8=-2\,(T3\cdot(X_0-T4)-R_0),$$

$$T9=Y_0^2+(X_0-T4)^2-R_0^2, \quad T10=T5^2-\left(1+T2^2\right)\cdot T7,$$

$$T11=2\cdot T5\cdot T6-\left(1+T2^2\right)\cdot T8, \quad T12=T6^2-\left(1+T2^2\right)\cdot T9,$$

with the condition $X_0\neq X_2$,
$(X_0,\ Y_0)$ being the coordinates of the center of side circle 0,
$(X_1,\ Y_1)$ being the coordinates of the center of middle circle 1,
$(X_2,\ Y_2)$ being the coordinates of the center of side circle 2,
R_0 being the radius of side circle 0,
R_1 being the radius of middle circle 1,
R_2 being the radius of side circle 2,
and $S=\pm1$, representing the two possible intersection points between T_0 and T_2.
To construct C-shaped triarcs within $\triangle ABC$, the sign of S must be chosen
such that the tangent points 4 and 5 lie within $\triangle ABC$.

A.2 Calculate the Generic Coordinates of the Tangent Points 4 and 5

For the **Type 1**, **Type 2**, and **Type 3** C-shaped triarcs, the relationship between the tangent point 4, the center (point 0) of side circle 0, the center (point 1) of middle circle 1, and the radii R_0 and R_1 is defined by this equation:

$$\frac{|\overrightarrow{\mathbf{04}}|}{|\overrightarrow{\mathbf{14}}|}=\frac{R_0}{R_1}, \quad \text{where } |\overrightarrow{\mathbf{14}}|>0 \text{ and } R_1>0. \tag{A-3}$$

From Eq. (A-3), the coordinates of tangent point 4 are derived as:

$$X_4 = \frac{R_1 \cdot X_0 - R_0 \cdot X_1}{R_1 - R_0}, \quad \text{where } R_1 \neq R_0; \tag{A-4a}$$

$$Y_4 = \frac{R_1 \cdot Y_0 - R_0 \cdot Y_1}{R_1 - R_0}, \quad \text{where } R_1 \neq R_0. \tag{A-4b}$$

For the **Type 1**, **Type 2**, and **Type 3** C-shaped triarcs, the relationship between the tangent point 5, the center (point 1) of middle circle 1, the center (point 2) of side circle 2, and the radii R_1 and R_2 is defined by this equation:

$$\frac{|\overrightarrow{\mathbf{25}}|}{|\overrightarrow{\mathbf{15}}|} = \frac{R_2}{R_1}, \quad \text{where } |\overrightarrow{\mathbf{15}}| > 0 \text{ and } R_1 > 0. \tag{A-5}$$

From Eq. (A-5), the coordinates of tangent point 5 are derived as:

$$X_5 = \frac{R_1 \cdot X_2 - R_2 \cdot X_1}{R_1 - R_2}, \quad \text{where } R_1 \neq R_2; \tag{A-6a}$$

$$Y_5 = \frac{R_1 \cdot Y_2 - R_2 \cdot Y_1}{R_1 - R_2}, \quad \text{where } R_1 \neq R_2. \tag{A-6b}$$

A.3 Determine the Boundary Radius R_{4b}

The boundary radius R_{4b} is the specific radius R_1 when middle circle 1 is tangent to side circle 0 at point A.

Combine Eqs. (A-2b) and (A-4a), have:

$$X_4 = \frac{(X_0 - T3 \cdot R_0) \cdot R_1 - R_0 \cdot T4 + T2 \cdot R_0 \cdot Y_1}{R_1 - R_0}, \quad \text{where } R_1 \neq R_0. \tag{A-7}$$

When the tangent point 4 coincides with point A, the following boundary conditions hold:

$$\left.\begin{aligned} \overrightarrow{\mathbf{AC}} \times \overrightarrow{\mathbf{C4}} = 0 \\ \overrightarrow{\mathbf{AB}} \times \overrightarrow{\mathbf{B4}} = 0 \end{aligned}\right\} \quad \text{when the tangent point 4 coincides with point A.} \tag{A-8}$$

Substitute $X_4 = X_A$ and $Y_4 = Y_A$ into Eqs. (A-7) and (A-4b), respectively, then obtain:

$$X_A \cdot (R_1 - R_0) = (X_0 - T3 \cdot R_0) \cdot R_1 - R_0 \cdot T4 + T2 \cdot R_0 \cdot Y_1; \tag{A-9a}$$

$$Y_A \cdot (R_1 - R_0) = R_1 \cdot Y_0 - R_0 \cdot Y_1, \tag{A-9b}$$

where

$(X_A,\ Y_A)$ are the coordinates of point A.

Multiply both sides of Eq. (A-9b) by T2, have:

$$T2 \cdot Y_A \cdot (R_1 - R_0) = T2 \cdot R_1 \cdot Y_0 - T2 \cdot R_0 \cdot Y_1. \tag{A-10}$$

Add Eqs. (A-9a) and (A-10) together, have R_{4b}:

$$X_A \cdot (R_1 - R_0) + T2 \cdot Y_A \cdot (R_1 - R_0) = R_1 \cdot (X_0 - T3 \cdot R_0) - R_0 \cdot T4 + R_1 \cdot Y_0 \cdot T2.$$

$$X_A \cdot R_1 - R_0 \cdot X_A + T2 \cdot Y_A \cdot R_1 - T2 \cdot Y_A \cdot R_0 = R_1 \cdot X_0 - T3 \cdot R_0 \cdot R_1 - R_0 \cdot T4 + R_1 \cdot Y_0 \cdot T2.$$

$$\therefore \quad R_{4b} = \frac{R_0 \cdot (X_A + T2 \cdot Y_A - T4)}{X_A + T2 \cdot Y_A + T3 \cdot R_0 - X_0 - Y_0 \cdot T2}, \tag{A-11}$$

where

$$T2 = \frac{Y_2 - Y_0}{X_2 - X_0}, \quad T3 = \frac{R_2 - R_0}{X_2 - X_0},$$
$$T4 = \frac{X_2^2 + Y_2^2 - R_2^2 + R_0^2 - X_0^2 - Y_0^2}{2(X_2 - X_0)},$$

with the condition $X_0 \neq X_2$,

$(X_0,\ Y_0)$ being the coordinates of the center of side circle 0,

$(X_2,\ Y_2)$ being the coordinates of the center of side circle 2,

$(X_A,\ Y_A)$ being the coordinates of point A,

R_0 being the radius of side circle 0, and R_2 being the radius of side circle 2.

A.4 Determine the Boundary Radius R_{5b}

The boundary radius R_{5b} is the specific radius R_1 when middle circle 1 is tangent to side circle 2 at point C. Combine Eqs. (A-2b) and (A-6a), have:

$$X_5 = \frac{(X_2 - T3 \cdot R_2) \cdot R_1 - R_2 \cdot T4 + T2 \cdot R_2 \cdot Y_1}{R_1 - R_2}, \quad \text{where } R_1 \neq R_2. \tag{A-12}$$

When the tangent point 5 coincides with point C, the following boundary conditions hold:

$$\left.\begin{aligned} \overrightarrow{\mathbf{CA}} \times \overrightarrow{\mathbf{A5}} = 0 \\ \overrightarrow{\mathbf{CB}} \times \overrightarrow{\mathbf{B5}} = 0 \end{aligned}\right\} \quad \text{when the tangent point 5 coincides with point C.} \tag{A-13}$$

Substitute $X_5 = X_C$ and $Y_5 = Y_C$ into Eqs. (A-12) and (A-6b), respectively, then obtain:

$$X_C \cdot (R_1 - R_2) = (X_2 - T3 \cdot R_2) \cdot R_1 - R_2 \cdot T4 + T2 \cdot R_2 \cdot Y_1; \tag{A-14a}$$
$$Y_C \cdot (R_1 - R_2) = R_1 \cdot Y_2 - R_2 \cdot Y_1, \tag{A-14b}$$

where

$(X_C,\ Y_C)$ are the coordinates of point C.

Multiply both sides of Eq. (A-14b) by T2, have:

$$T2 \cdot Y_C \cdot (R_1 - R_2) = T2 \cdot R_1 \cdot Y_2 - T2 \cdot R_2 \cdot Y_1. \tag{A-15}$$

Add Eqs. (A-14a) and (A-15) together, have R_{5b}:

$$X_C \cdot (R_1 - R_2) + T2 \cdot Y_C \cdot (R_1 - R_2) = R_1 \cdot (X_2 - T3 \cdot R_2) - R_2 \cdot T4 + R_1 \cdot Y_2 \cdot T2.$$
$$X_C \cdot R_1 - R_2 \cdot X_C + T2 \cdot Y_C \cdot R_1 - T2 \cdot Y_C \cdot R_2 = R_1 \cdot X_2 - T3 \cdot R_2 \cdot R_1 - R_2 \cdot T4 + R_1 \cdot Y_2 \cdot T2.$$

$$\therefore \quad R_{5b} = \frac{R_2 \cdot (X_C + T2 \cdot Y_C - T4)}{X_C + T2 \cdot Y_C + T3 \cdot R_2 - X_2 - Y_2 \cdot T2}, \tag{A-16}$$

where

$$T2 = \frac{Y_2 - Y_0}{X_2 - X_0}, \quad T3 = \frac{R_2 - R_0}{X_2 - X_0},$$
$$T4 = \frac{X_2^2 + Y_2^2 - R_2^2 + R_0^2 - X_0^2 - Y_0^2}{2(X_2 - X_0)},$$

with the condition $X_0 \neq X_2$,

$(X_0,\ Y_0)$ being the coordinates of the center of side circle 0,

$(X_2,\ Y_2)$ being the coordinates of the center of side circle 2,

$(X_C,\ Y_C)$ being the coordinates of point C,

R_0 being the radius of side circle 0, and R_2 being the radius of side circle 2.

B APPENDIX: SUPPORTING LEMMAS

Several lemmas are introduced to derive the equations for the radius R_1 and to prove the approach properties (strict, anti-strict, advanced, and anti-advanced) of the C-shaped triarcs within $\triangle ABC$.

This section applies the equations established in Appendix A. For convenience, the general coordinate system in Fig. A.1 is transformed to a special coordinate system (Fig. B.1) in which the center 0 of side circle 0 is placed at the origin, and the center 2 of side circle 2 lies on the positive X-axis.

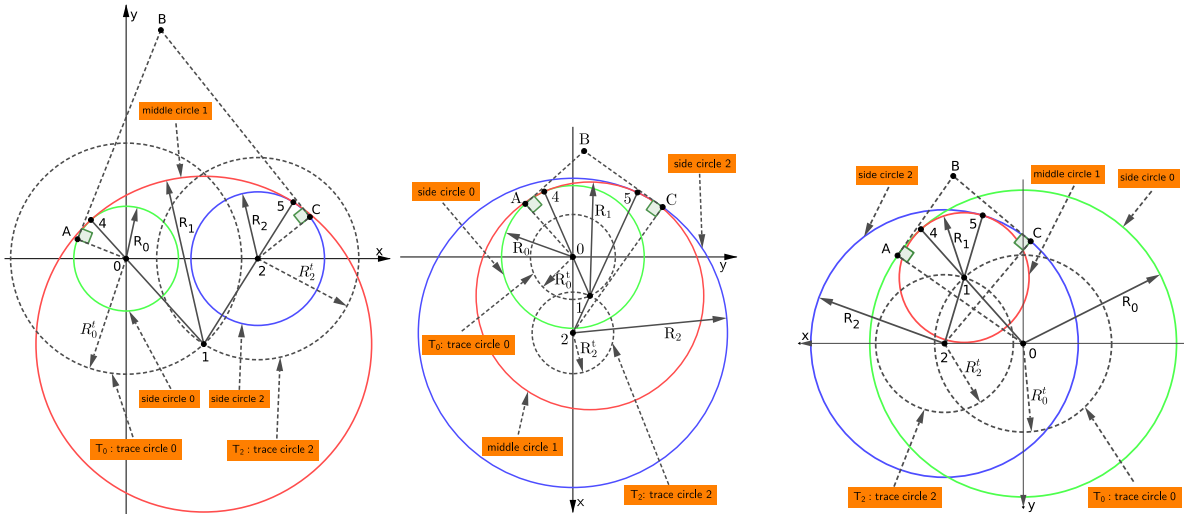

(a) **Type 1** (b) **Type 2** (c) **Type 3**

Figure B.1: R_1 construction in the special coordinate system. Panels correspond to the configurations in Appendix A (Fig. A.1) but rotated/transformed so center 0 is at the origin and center 2 is on the positive X-axis. Full definitions and notation are in Appendix A.

By substituting $X_0 = 0$, $Y_0 = 0$, and $Y_2 = 0$ into Eqs. (A-2a), (A-2b), (A-4a), (A-4b), (A-6a), and (A-6b), the coordinates of the center $1(X_1, Y_1)$, the tangent point $4(X_4, Y_4)$, and the tangent point $5(X_5, Y_5)$ simplify

to:

$$X_1 = \frac{X_2}{2} + \frac{(R_0 - R_2)(R_0 + R_2 - 2R_1)}{2X_2}, \quad \text{where } X_2 > 0. \tag{B-1a}$$

$$Y_1 = S\sqrt{(R_0 - R_1)^2 - X_1^2} \quad \begin{cases} (R_0 - R_1)^2 - X_1^2 = 0, & \text{if point 1 lies on the positive } X\text{-axis;} \\ (R_0 - R_1)^2 - X_1^2 > 0, & \text{otherwise,} \\ & \text{where } S = \pm 1. \end{cases} \tag{B-1b}$$

$$X_4 = -\frac{R_0 \cdot X_1}{R_1 - R_0}, \quad \text{where } R_1 \neq R_0. \tag{B-2a}$$

$$Y_4 = -\frac{R_0 \cdot Y_1}{R_1 - R_0}, \quad \text{where } R_1 \neq R_0. \tag{B-2b}$$

$$X_5 = \frac{R_1 \cdot X_2 - R_2 \cdot X_1}{R_1 - R_2}, \quad \text{where } R_1 \neq R_2. \tag{B-3a}$$

$$Y_5 = -\frac{R_2 \cdot Y_1}{R_1 - R_2}, \quad \text{where } R_1 \neq R_2. \tag{B-3b}$$

B.1 Lemmas for the Coordinate X_4 of the Tangent Point 4

By substituting X_1 from Eq. (B-1a) into Eq. (B-2a), the first derivative of X_4 with respect to R_1 in Eq. (B-2a) is:

$$\frac{dX_4}{dR_1} = \frac{R_0 \cdot \left(X_2^2 - (R_0 - R_2)^2\right)}{2X_2 \cdot (R_1 - R_0)^2}, \quad \text{where } R_1 \neq R_0 \text{ and } X_2 > 0. \tag{B-4}$$

The analysis of Eq. (B-4) leads to the following lemmas:

Lemma B.1. *For **Type 1** C-shaped triarcs, given that X_2, R_0, and R_2 are fixed, the coordinate X_4 of the tangent point 4 is a strictly increasing function with respect to the variable R_1 that is the radius of middle circle 1.*

Proof. For **Type 1** C-shaped triarcs (Fig. B.1a),
$\because X_2 > 0$,
$\because$ both side circles 0 and 2 are either separated, tangent externally, or intersecting, $\Longrightarrow X_2^2 - (R_0 - R_2)^2 > 0$,
$\therefore \frac{dX_4}{dR_1} > 0$. □

Lemma B.2. *For **Type 2** C-shaped triarcs, given that X_2, R_0, and R_2 are fixed, the coordinate X_4 of the tangent point 4 is a strictly decreasing function with respect to the variable R_1 that is the radius of middle circle 1.*

Proof. For **Type 2** C-shaped triarcs (Fig. B.1b),
$\because X_2 > 0$,
$\because$ side circle 0 is inside side circle 2, $\Longrightarrow X_2^2 - (R_0 - R_2)^2 < 0$,
$\therefore \frac{dX_4}{dR_1} < 0$. □

Lemma B.3. *For **Type 3** C-shaped triarcs, given that X_2, R_0, and R_2 are fixed, the coordinate X_4 of the tangent point 4 is a strictly increasing function with respect to the variable R_1 that is the radius of middle circle 1.*

Proof. For **Type 3** C-shaped triarcs (Fig. B.1c),
$\because X_2 > 0$,
$\because$ both side circles 0 and 2 are intersecting, $\Longrightarrow X_2^2 - (R_0 - R_2)^2 > 0$,
$\therefore \frac{dX_4}{dR_1} > 0$. □

B.2 Lemmas for the Coordinate X_5 of the Tangent Point 5

By substituting X_1 from Eq. (B-1a) into Eq. (B-3a), the first derivative of X_5 with respect to R_1 in Eq. (B-3a) is:

$$\frac{dX_5}{dR_1} = \frac{R_2 \cdot \left((R_0 - R_2)^2 - X_2^2\right)}{2X_2 \cdot (R_1 - R_2)^2}, \quad \text{where } R_1 \neq R_2 \text{ and } X_2 > 0. \tag{B-5}$$

The analysis of Eq. (B-5) leads to the following lemmas:

Lemma B.4. *For **Type 1** C-shaped triarcs, given that X_2, R_0, and R_2 are fixed, the coordinate X_5 of the tangent point 5 is a strictly decreasing function with respect to the variable R_1 that is the radius of middle circle 1.*

Proof. For **Type 1** C-shaped triarcs (Fig. B.1a),
$\because X_2 > 0$,
$\because$ both side circles 0 and 2 are either separated, tangent externally, or intersecting, $\Longrightarrow (R_0 - R_2)^2 - X_2^2 < 0$,
$\therefore \frac{dX_5}{dR_1} < 0$. □

Lemma B.5. *For **Type 2** C-shaped triarcs, given that X_2, R_0, and R_2 are fixed, the coordinate X_5 of the tangent point 5 is a strictly increasing function with respect to the variable R_1 that is the radius of middle circle 1.*

Proof. For **Type 2** C-shaped triarcs (Fig. B.1b),
$\because X_2 > 0$,
$\because$ side circle 0 is inside side circle 2, $\Longrightarrow (R_0 - R_2)^2 - X_2^2 > 0$,
$\therefore \frac{dX_5}{dR_1} > 0$. □

Lemma B.6. *For **Type 3** C-shaped triarcs, given that X_2, R_0, and R_2 are fixed, the coordinate X_5 of the tangent point 5 is a strictly decreasing function with respect to the variable R_1 that is the radius of middle circle 1.*

Proof. For **Type 3** C-shaped triarcs (Fig. B.1c),
$\because X_2 > 0$,
$\because$ both side circles 0 and 2 are intersecting, $\Longrightarrow (R_0 - R_2)^2 - X_2^2 < 0$,
$\therefore \frac{dX_5}{dR_1} < 0$. □

C APPENDIX: VECTOR-BASED IMPLEMENTATION FORMULATION

To facilitate practical implementation in software environments, the triarc construction is formulated using vector operations. Let $\mathbf{A}, \mathbf{B}, \mathbf{C} \in \mathbb{R}^2$ be the position vectors of the triangle vertices. We define the normalized edge directions as:

$$\mathbf{t}_0 = \frac{\mathbf{B} - \mathbf{A}}{|\mathbf{B} - \mathbf{A}|}, \quad \mathbf{t}_2 = \frac{\mathbf{C} - \mathbf{B}}{|\mathbf{C} - \mathbf{B}|}$$

Side Arc Centers and Normals

Under the clockwise (CW) triangle orientation assumed in this work ($\mathbf{AB} \times \mathbf{BC} < 0$), the triangle interior lies to the right of the directed edges. Consequently, the inward unit normals $\mathbf{n}_i$ are obtained via a 90° clockwise rotation of the tangents:

$$\mathbf{n}_0 = \begin{bmatrix} 0 & 1 \\ -1 & 0 \end{bmatrix} \mathbf{t}_0, \quad \mathbf{n}_2 = \begin{bmatrix} 0 & 1 \\ -1 & 0 \end{bmatrix} \mathbf{t}_2$$

The side arc centers are then directly computed using the radii R_0 and R_2 (derived in Section 2.2):

$$\mathbf{O}_0 = \mathbf{A} + R_0 \mathbf{n}_0, \quad \mathbf{O}_2 = \mathbf{C} + R_2 \mathbf{n}_2$$

Numerical Robustness and Degeneracy

The vector-based formulation allows for robust detection of nearly collinear configurations using the cross product $D = \mathbf{BA} \times \mathbf{BC}$ and the dot product $P = \mathbf{BA} \cdot \mathbf{BC}$ of the control edges.

If $|D| < \varepsilon$ and $P < 0$, the vectors are nearly anti-parallel ($\angle B \approx 180°$). In this "nearly flat" situation, the algorithm collapses the triarc into a single linear segment **AC** to maintain numerical stability and avoid the calculation of singular radii.

If $|D| < \varepsilon$ and $P > 0$, the triangle forms a "nearly needle" configuration ($\angle B \approx 0°$). The handling of this degeneracy depends on the triarc type:

- For **Types 1 and 2**, the geometry is simplified to a linear segment **AC**.
- For **Type 3**, the construction results in a fractional polyline ABC. The length of this needle approximation is determined by the magnitude of the approach coefficients α_i; as $\alpha_i \to \infty$, the output converges to the full control polyline ABC.

This categorical handling ensures that the implementation remains robust in software environments where control points may be nearly collinear.

Middle Arc Center and Junction Points

The middle arc center $\mathbf{O}_1$ is determined by the intersection of two locus circles centered at the side centers $\mathbf{O}_0$ and $\mathbf{O}_2$. For a C-shaped triarc with internal tangencies, the radii of these locus circles are $L_0 = |R_1 - R_0|$ and $L_2 = |R_1 - R_2|$, respectively. The center $\mathbf{O}_1$ is found by solving for the intersection of:

$$|\mathbf{O}_1 - \mathbf{O}_0|^2 = L_0^2, \quad |\mathbf{O}_1 - \mathbf{O}_2|^2 = L_2^2$$

Defining $\mathbf{D} = \mathbf{O}_2 - \mathbf{O}_0$ and $d = |\mathbf{D}|$, the coordinates of $\mathbf{O}_1$ relative to $\mathbf{O}_0$ are:

$$\mathbf{O}_1 = \mathbf{O}_0 + \frac{a}{d}\mathbf{D} \pm \frac{h}{d}\mathbf{D}^{\perp}$$

where $\mathbf{D}^{\perp}$ denotes a 90° rotation of $\mathbf{D}$ consistent with the triangle orientation, $a = (L_0^2 - L_2^2 + d^2)/(2d)$, and $h = \sqrt{L_0^2 - a^2}$. The sign of the $\mathbf{D}^{\perp}$ term is chosen to ensure that Inequalities 15 hold, so that the triarc remains within the control triangle ABC.

Once $\mathbf{O}_1$ is determined, the junction points $\mathbf{P}_4$ and $\mathbf{P}_5$ are uniquely obtained by projecting the radii onto the lines connecting the centers:

$$\mathbf{P}_4 = \mathbf{O}_0 + s_0 \frac{R_0}{|\mathbf{O}_1 - \mathbf{O}_0|}(\mathbf{O}_1 - \mathbf{O}_0), \quad \mathbf{P}_5 = \mathbf{O}_2 + s_2 \frac{R_2}{|\mathbf{O}_1 - \mathbf{O}_2|}(\mathbf{O}_1 - \mathbf{O}_2)$$

where the orientation signs s_i are defined according to the contact geometry of each type:

- **Type 1:** $s_0 = -1, s_2 = -1$.
- **Type 2:** $s_0 = -1, s_2 = 1$.
- **Type 3:** $s_0 = 1, s_2 = 1$.

Final Triarc Representation

The resulting triarc is uniquely defined by the triplet of centers $\{\mathbf{O}_0, \mathbf{O}_1, \mathbf{O}_2\}$, the corresponding radii $\{R_0, R_1, R_2\}$, and the connection points $\{\mathbf{A}, \mathbf{P}_4, \mathbf{P}_5, \mathbf{C}\}$.

REFERENCES

[1] Banchoff, T.; Giblin, P.: On the geometry of piecewise circular curves. The American Mathematical Monthly, 101(5), 1994, 403–416. https://doi.org/10.1080/00029890.1994.11996965.

[2] Bertolazzi, E.; Frego, M.: A note on robust Biarc computation. Computer-Aided Design and Applications, 16(5), 2019, 822–835. https://doi.org/10.14733/cadaps.2019.822-835.

[3] Bolton, K.M.: Biarc curves. Computer-Aided Design, 7(2), 1975, 89–92. https://doi.org/10.1016/0010-4485(75)90086-X.

[4] Chandrupatla, T.R.; Osler, T.J.: Planar Biarc curves: A geometric view. The Mathematical Scientist, 36(2), 2011, 117–125.

[5] Jakubczyk, K.: Approximation of smooth planar curves by circular arc splines. Information Systems and Technologies, 2012, 203–214. Initially appeared as a Technical Report in 2010.

[6] Knez, M.; Peternell, M.; Alcázar, J.G.: From theoretical to applied geometry – recent developments. Computer Aided Geometric Design, 81, 2020, 101912. https://doi.org/10.1016/j.cagd.2020.101912.

[7] Meek, D.S.; Walton, D.J.: Approximating smooth planar curves by arc splines. Journal of Computational and Applied Mathematics, 59(2), 1995, 221–231. https://doi.org/10.1016/0377-0427(94)00029-Z.

[8] Piegl, L.A.; Tiller, W.: Data approximation using Biarcs. Engineering with Computers, 18(1), 2002, 59–65. https://doi.org/10.1007/s003660200005.

[9] Yang, M.Y.; Shon, T.Y.; Lee, T.M.; Lee, T.M.: Cam profile machining by triarc curve fitting. International Journal of Production Research, 36(7), 1998, 1767–1778. https://doi.org/10.1080/002075498192959.